



Article

Halogen Bond to Experimentally Significant N-Heterocyclic Carbenes (I, IMe₂, IⁱPr₂, I^tBu₂, IPh₂, IMes₂, IDipp₂, IAd₂; I = Imidazol-2-ylidene)

Mirosław Jabłoński

Faculty of Chemistry, Nicolaus Copernicus University in Toruń, Gagarina 7, 87-100 Torun, Poland; teojab@chem.umk.pl; Tel.: +48-056-611-4695

Abstract: The subjects of the article are halogen bonds between either XCN or XCCH (X = Cl, Br, I) and the carbene carbon atom in imidazol-2-ylidene (I) or its derivatives (IR₂) with experimentally significant and systematically increased R substituents at both nitrogen atoms: methyl = Me, *iso*-propyl = ⁱPr, *tert*-butyl = ^tBu, phenyl = Ph, mesityl = Mes, 2,6-diisopropylphenyl = Dipp, 1-adamantyl = Ad. It is shown that the halogen bond strength increases in the order Cl < Br < I and the XCN molecule forms stronger complexes than XCCH. Of all the carbenes considered, IMes₂ forms the strongest and also the shortest halogen bonds with an apogee for complex IMes₂ ··· ICN for which $D_0 = 18.71$ kcal/mol and $d_{C...I} = 2.541$ Å. In many cases, IDipp₂ forms as strong halogen bonds as IMes₂. Quite the opposite, although characterized by the greatest nucleophilicity, I^tBu₂ forms the weakest complexes (and the longest halogen bonds) if X ≠ Cl. While this finding can easily be attributed to the steric hindrance exerted by the highly branched *tert*-butyl groups, it appears that the presence of the four C-H ··· X hydrogen bonds may also be of importance here. Similar situation occurs in the case of complexes with IAd₂.

Keywords: carbene; N-heterocyclic carbene; NHC; halogen bond; XB; intermolecular interaction; steric effect; spatial hindrance



Citation: Jabłoński, M. Halogen Bond to Experimentally Significant N-Heterocyclic Carbenes (I, IMe₂, IⁱPr₂, I^tBu₂, IPh₂, IMes₂, IDipp₂, IAd₂; I = Imidazol-2-ylidene). *Int. J. Mol. Sci.* **2023**, *24*, 9057. <https://doi.org/10.3390/ijms24109057>

Academic Editor: Alexander Novikov

Received: 24 April 2023

Revised: 15 May 2023

Accepted: 18 May 2023

Published: 21 May 2023



Copyright: © 2023 by the author. Licensee MDPI, Basel, Switzerland. This article is an open access article distributed under the terms and conditions of the Creative Commons Attribution (CC BY) license (<https://creativecommons.org/licenses/by/4.0/>).

1. Introduction

Carbenes [1–10], especially the N-heterocyclic (NHC) [11–23] ones, are of fundamental importance in organic and organometallic chemistry as well as in homogeneous catalysis [24–35], material chemistry [36,37], and medicine [38,39]. The imidazol-2-ylidene derivatives are especially important in this respect. The significant reactivity of these derivatives and other NHCs results from the presence of a lone electron pair on the carbene carbon atom, which makes these carbenes good nucleophilic reagents. In this respect, carbenes are most often considered electron charge donors, i.e., Lewis bases, in combination with transition metal atoms, usually forming strong complexes [40–56]. However, the carbene carbon atom readily forms contacts with atoms other than transition metals as well, forming hydrogen bonds [57–65], lithium bonds [66–68], beryllium bonds [69–72], magnesium bonds [73–75], triel bonds [76–79], tetrel bonds [80–82], pnictogen bonds [83–85], chalcogen bonds [86], halogen bonds [87–95], and even aerogen bonds [96]. However, it is worth mentioning here that in addition to the nucleophilic properties of carbenes resulting from the presence of a lone electron pair on the carbene carbon atom, singlet carbenes [97–103] also exhibit electrophilic properties [104–109] associated with the presence of an empty *p*-orbital perpendicular to the plane of the molecule. Although the target of electrophilic attack is most often nitrogen or phosphorus [105], it has recently been shown that the carbene carbon atom can also interact with the Si-H bond in silane to form a specific type of tetrel bond [107–109].

The subject of this article is a special case of the halogen bond, because the donor of the lone electron pair is the carbene carbon atom and not, as in most cases, a strongly

electronegative atom such as, e.g., N, P, O, S, or another halogen [110–113]. Thus, the carbene molecule here is a Lewis base, while the molecule with the contacting halogen atom acting through the σ -hole [114–118] is a Lewis acid. The first adduct related to the interaction between the carbene carbon atom and the halogen atom was obtained by Arduengo III et al. [87] in 1991. It was formed by the reaction of 1,3-di-1-adamantyl-imidazol-2-ylidene (IAd₂) with iodopentafluorobenzene. Subsequently, Kuhn et al. [88] obtained a stable carbene iodine adduct by reacting 1,3-diethyl-4,5-dimethylimidazol-2-ylidene with iodine. These two examples clearly show that iodine is the best halogen atom as an electron pair acceptor. This is, of course, due to the fact that the σ -hole is particularly well developed on the iodine atom. The first theoretical studies of the halogen bond involving a carbene molecule were made by Li et al. [89] only in 2009. Namely, they performed calculations for five complexes H₂C···BrH, F₂C···BrH, Me₂C···BrH, H₂C···BrCCH, and H₂C···BrCN. It was not until 2013 that Esrafilii and Mohammadirad studied the H₂C···XCXY (X = Cl, Br, I; Y = H, F, COF, COOH, CF₃, NO₂, CN, NH₂, CH₃, OH) complexes [90] and the H₂C···XCN···XCN linear trimers (X = F, Cl, Br, I) [91]. As can be seen, the first three computational works concerned the simplest carbene CH₂, i.e., methylene, or its simple derivatives. Only in 2014, Donoso-Tauda et al. [92] performed calculations for complexes involving 1,3-dimethylimidazole-2-ylidene (IMe₂). The donors of the X halogen atom (X = Cl, Br) were X-A molecules, where A = F, Cl, Br, CN, CCH, CF₃, CH₃ or H. Dimers between XCN (X = Cl, Br, I) and imidazol-2-ylidene derivatives, including, e.g., 1,3-di-*tert*-butyl-imidazole-2-ylidene (*t*Bu₂) and 1,3-diphenylimidazole-2-ylidene (IPh₂) were studied in the same year by Lv et al. [93]. Then, Del Bene et al. [94] performed theoretical studies of the halogen bond between ClCCH, ClCN, ClNC, or ClF and some rather exotic small carbenes. Quite recently, Grabowski performed calculations for imidazol-2-ylidene complexes with XCCH, XCN, and X₂ (X = F, Cl, Br, I) [95]. As might be expected, the F molecules did not form a halogen bond to the carbene carbon atom. In addition to the aforementioned work on halogen bonds involving carbenes, it is also worth mentioning the recent theoretical article by Sanyal and Esterhuysen [119] on halogen bonds involving carbones and the hot paper on halogen complexes of anionic NHCs by Frosch et al. [120].

The examples cited [89–95] clearly show that currently there is practically no theoretical work on halogen bonding involving larger and experimentally significant NHC-type carbenes. In the vast majority of cases, these are derivatives of imidazol-2-ylidene containing large groups at both nitrogens of the heterocycle, e.g., 1-adamantyl (= Ad), 2,6-diisopropylphenyl (= Dipp), mesityl (= Mes), *tert*-butyl (= *t*Bu), or *iso*-propyl (= *i*Pr). It is enough to recall here that the first adduct of the carbene and halogen compound was a derivative of 1,3-di-1-adamantyl-imidazol-2-ylidene (IAd₂) [87]. Unfortunately, calculations with such large substituents are computationally very expensive. Nevertheless, the aim of this article is to systematically investigate the characteristics of the halogen bond between the most popular halogen donors XCCH and XCN (X = Cl, Br, I) and the carbene carbon atom of the experimentally significant imidazol-2-ylidene derivatives. Additionally, imidazol-2-ylidene itself and its several smaller derivatives are also investigated. Thus, the considered carbenes are imidazol-2-ylidene (I) and its derivatives (IR₂) with progressively larger substituents (R) at the heterocyclic nitrogens: methyl = Me, *iso*-propyl = *i*Pr, *tert*-butyl = *t*Bu, phenyl = Ph, mesityl = Mes, 2,6-diisopropylphenyl = Dipp, 1-adamantyl = Ad. The general form of the considered IR₂···XD complexes is shown in Figure 1. Of particular interest is the structure of the obtained complexes IR₂···XCN and IR₂···XCCH, as well as the characteristics of the halogen bonds that hold them together.

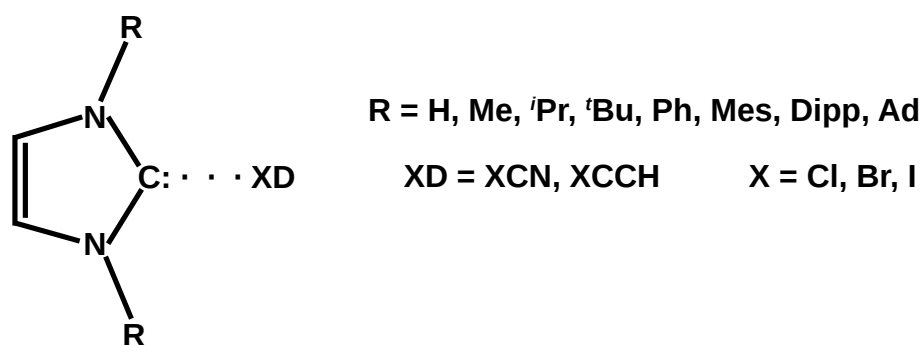


Figure 1. General scheme of the $\text{IR}_2 \cdots \text{XD}$ complexes ($R = \text{H, Me, } ^i\text{Pr, } ^t\text{Bu, Ph, Mes, Dipp, Ad}$; $XD = \text{XCN, XCCH}$; $X = \text{Cl, Br, I}$). The colon on the carbene carbon atom represents a lone electron pair.

2. Results and Discussion

2.1. Nucleophilicity of Carbenes

Before discussing the results of the analyzed complexes, it is worth first quantifying the nucleophilicity index, N , of the individual carbenes, as nucleophilicity measures the ability of a nucleophile to react at an electron-deficient center [121] and therefore will be useful in the initial estimation of the tendency of a given carbene to form a halogen bond. Unfortunately, in the literature, one can find several expressions for the nucleophilicity index. Therefore, four methods were used to determine it (Method I-IV, see the Methodology section) [122]. The obtained values are presented in Table 1.

Table 1. Nucleophilicity index of the analyzed carbenes.

| Method | Molecule | | | | | | | |
|--------|----------|------------------|--------------------------------|--------------------------------|------------------------------|-------------------|--------------------|------------------|
| | I | IMe ₂ | I ⁱ Pr ₂ | I ^t Bu ₂ | I ^{Ph} ₂ | IMes ₂ | IDipp ₂ | IAd ₂ |
| I | 3.27 | 3.39 | 3.42 | 3.63 | 3.28 | 3.37 | 3.84 | 3.24 |
| II | 1.22 | 1.30 | 1.31 | 1.36 | 1.28 | 1.30 | 1.25 | 1.32 |
| III | 2.54 | 2.67 | 2.74 | 2.84 | 2.67 | 2.75 | 2.89 | 2.72 |
| IV | 2.39 | 2.53 | 2.58 | 2.68 | 2.52 | 2.58 | 2.68 | 2.53 |

The nucleophilicity index values obtained suggest that I (i.e., imidazol-2-ylidene) should have the lowest tendency to form a halogen bond, while I^tBu₂ and IDipp₂, on the contrary, should have the highest. It is worth noting that the nucleophilicity index clearly increased with the increase of the aliphatic substituent, e.g., in the case of Method III (it has been shown [122] that this method is superior to Method IV and especially I and II) we have: I (2.54) < IMe₂ (2.67) < IⁱPr₂ (2.74) < I^tBu₂ (2.84). Similarly, the insertion of three methyl groups or two *iso*-propyl groups into the side phenyl group also led to an increase in the nucleophilicity index value: I (2.54) < I^{Ph}₂ (2.67) < IMes₂ (2.75) < IDipp₂ (2.89). Most likely, these trends can be explained by the increase in the inductive effect (+I). However, the values of the obtained nucleophilicity indices did not fully transform into the strength of the obtained halogen bonds (*vide infra*).

2.2. Characteristics of $\text{IR}_2 \cdots \text{XCCN}$ and $\text{IR}_2 \cdots \text{XCN}$ Dimers

Undoubtedly, the most important parameters describing halogen bonds in the $\text{IR}_2 \cdots \text{XCCH}$, and $\text{IR}_2 \cdots \text{XCN}$ ($X = \text{Cl, Br, I}$) complexes are the dissociation energy (D_0), the halogen bond length ($d_{\text{C}\cdots\text{X}}$), and the C-X-C angle (α_{CXC}). The values of these parameters are shown in Table 2. In addition, this table also contains the values of the most important QTAIM [123] quantities: the electron density ($\rho_{\text{C}\cdots\text{X}}$) and its Laplacian ($\nabla^2\rho_{\text{C}\cdots\text{X}}$) and the total electronic energy density ($H_{\text{C}\cdots\text{X}}$) determined at the bond critical point of the $\text{C}\cdots\text{X}$ halogen bond.

Table 2. Dissociation energy (D_0 in kcal/mol), halogen bond length ($d_{C\dots X}$ in Å), C-X-C angle (α_{CXC} in degrees), electron density ($\rho_{C\dots X}$ in a.u.), Laplacian of the electron density ($\nabla^2\rho_{C\dots X}$ in a.u.), and the total electronic energy density ($H_{C\dots X}$ in a.u.) obtained for the $IR_2 \cdots XCCH$ and $IR_2 \cdots XCN$ ($X = Cl, Br, I$) complexes.

| X-Donor | Parameters | Carbene | | | | | | | |
|---------|---------------------------|---------|------------------|--------------------------------|--------------------------------|------------------|-------------------|--------------------|------------------|
| | | I | IMe ₂ | I ⁱ Pr ₂ | I ^t Bu ₂ | IPh ₂ | IMes ₂ | IDipp ₂ | IAd ₂ |
| ClCN | D_0 | 5.87 | 6.63 | 6.99 | 6.11 | 6.99 | 9.26 | 8.59 | 6.78 |
| | $d_{C\dots X}$ | 2.979 | 2.959 | 2.955 | 3.144 | 2.959 | 3.168 | 3.019 | 3.138 |
| | α_{CXC} | 180.0 | 180.0 | 180.0 | 180.0 | 179.4 | 152.9 | 171.7 | 180.0 |
| | $\rho_{C\dots X}$ | 0.016 | 0.017 | 0.017 | 0.012 | 0.016 | 0.011 | 0.014 | 0.012 |
| | $\nabla^2\rho_{C\dots X}$ | 0.050 | 0.052 | 0.052 | 0.037 | 0.052 | 0.035 | 0.045 | 0.038 |
| | $H_{C\dots X}$ | 0.0015 | 0.0014 | 0.0014 | 0.0012 | 0.0014 | 0.0013 | 0.0014 | 0.0013 |
| BrCN | D_0 | 8.58 | 9.59 | 10.00 | 7.23 | 9.37 | 11.18 | 10.95 | 7.84 |
| | $d_{C\dots X}$ | 2.877 | 2.843 | 2.829 | 3.148 | 2.887 | 2.830 | 2.856 | 3.143 |
| | α_{CXC} | 180.0 | 180.0 | 180.0 | 180.0 | 179.2 | 176.2 | 177.0 | 180.0 |
| | $\rho_{C\dots X}$ | 0.022 | 0.024 | 0.025 | 0.014 | 0.022 | 0.025 | 0.023 | 0.014 |
| | $\nabla^2\rho_{C\dots X}$ | 0.061 | 0.063 | 0.064 | 0.039 | 0.060 | 0.065 | 0.062 | 0.039 |
| | $H_{C\dots X}$ | 0.0009 | 0.0005 | 0.0004 | 0.0011 | 0.0008 | 0.0006 | 0.0007 | 0.0012 |
| ICN | D_0 | 14.31 | 16.18 | 17.12 | 9.71 | 14.81 | 18.71 | 17.56 | 10.54 |
| | $d_{C\dots X}$ | 2.640 | 2.589 | 2.552 | 3.162 | 2.703 | 2.541 | 2.601 | 3.152 |
| | α_{CXC} | 180.0 | 180.0 | 178.2 | 180.0 | 177.8 | 179.4 | 180.0 | 180.0 |
| | $\rho_{C\dots X}$ | 0.044 | 0.049 | 0.052 | 0.017 | 0.039 | 0.053 | 0.047 | 0.017 |
| | $\nabla^2\rho_{C\dots X}$ | 0.074 | 0.073 | 0.073 | 0.041 | 0.071 | 0.075 | 0.073 | 0.041 |
| | $H_{C\dots X}$ | −0.0064 | −0.0089 | −0.0108 | 0.0006 | −0.0044 | −0.0109 | −0.0083 | 0.0006 |
| ClCCH | D_0 | 3.43 | 4.02 | 4.29 | 3.93 | 4.33 | 5.97 | 5.90 | 4.47 |
| | $d_{C\dots X}$ | 3.042 | 3.062 | 3.060 | 3.279 | 3.069 | 3.359 | 3.235 | 3.284 |
| | α_{CXC} | 165.9 | 180.0 | 180.0 | 180.0 | 179.3 | 154.6 | 164.3 | 180.0 |
| | $\rho_{C\dots X}$ | 0.013 | 0.014 | 0.014 | 0.010 | 0.013 | 0.008 | 0.010 | 0.009 |
| | $\nabla^2\rho_{C\dots X}$ | 0.043 | 0.044 | 0.044 | 0.030 | 0.043 | 0.024 | 0.030 | 0.029 |
| | $H_{C\dots X}$ | 0.0014 | 0.0014 | 0.0014 | 0.0012 | 0.0014 | 0.0011 | 0.0012 | 0.0012 |
| BrCCH | D_0 | 5.30 | 6.16 | 6.40 | 4.70 | 6.09 | 7.34 | 7.39 | 5.32 |
| | $d_{C\dots X}$ | 3.023 | 3.004 | 2.996 | 3.319 | 3.039 | 2.999 | 3.006 | 3.324 |
| | α_{CXC} | 177.4 | 180.0 | 180.0 | 180.0 | 179.9 | 174.8 | 177.2 | 180.0 |
| | $\rho_{C\dots X}$ | 0.017 | 0.018 | 0.018 | 0.010 | 0.017 | 0.017 | 0.017 | 0.010 |
| | $\nabla^2\rho_{C\dots X}$ | 0.049 | 0.051 | 0.051 | 0.029 | 0.048 | 0.051 | 0.051 | 0.029 |
| | $H_{C\dots X}$ | 0.0013 | 0.0012 | 0.0012 | 0.0011 | 0.0012 | 0.0013 | 0.0013 | 0.0011 |
| ICCH | D_0 | 9.15 | 10.47 | 11.01 | 6.62 | 9.77 | 12.05 | 11.66 | 7.35 |
| | $d_{C\dots X}$ | 2.902 | 2.861 | 2.827 | 3.372 | 2.951 | 2.822 | 2.884 | 3.371 |
| | α_{CXC} | 178.7 | 180.0 | 177.7 | 180.0 | 178.3 | 177.9 | 179.5 | 180.0 |
| | $\rho_{C\dots X}$ | 0.026 | 0.029 | 0.031 | 0.012 | 0.024 | 0.030 | 0.027 | 0.012 |
| | $\nabla^2\rho_{C\dots X}$ | 0.063 | 0.065 | 0.066 | 0.030 | 0.059 | 0.068 | 0.064 | 0.030 |
| | $H_{C\dots X}$ | −0.0004 | −0.0012 | −0.0017 | 0.0009 | 0.0000 | −0.0016 | −0.0007 | 0.0009 |

As expected for a given X-donor molecule, the halogen bond strength increases in the order of $Cl < Br < I$. For example, for the simplest $I \cdots XCN$ complexes, the D_0 values are 5.87, 8.58, and 14.31 kcal/mol, respectively, and for the $IDipp_2 \cdots XCN$ complexes, the values are 8.59, 10.95, and 17.56 kcal/mol. It is also seen that XCN molecules form stronger complexes with carbenes than XCCH, which proves that XCN are much better halogen donors.

However, it is more interesting to consider the strength of the complexes depending on the type of IR_2 carbene molecule. As shown in the previous subsection (Table 1), the nucleophilicity index values determined suggest that unsubstituted imidazol-2-ylidene

should form the weakest halogen bonds, while I^tBu_2 and $IDipp_2$ the strongest. Therefore, the D_0 values shown in Table 2 may seem surprising at first. Namely, although in the case of the halogen donors $ClCN$ and $ClCCH$, imidazol-2-ylidene (**I**) indeed forms the weakest complexes (5.87 and 3.43 kcal/mol, respectively), in the case of the other halogen donors, the carbene I^tBu_2 gives the weakest and not the strongest complexes (e.g., in the case of $I^tBu_2 \cdots BrCCH$ the D_0 value is only 4.70 kcal/mol while for $I \cdots BrCCH$ it is 5.30 kcal/mol and for $IAd_2 \cdots BrCCH$ it amounts to 5.32 kcal/mol). Moreover, the halogen bond length ($d_{C \cdots X}$) values presented in Table 2 clearly show that I^tBu_2 forms the longest halogen bond in most cases, with XCN over 3.14 Å and with $XCCH$ over 3.28 Å. At the same time, the halogen bonds formed by this carbene are always linear. What is more, the halogen bonds formed by I^tBu_2 (as well as IAd_2) are characterized by the smallest values of the electron density at the $C \cdots X$ bond critical point. For example, in the $I^tBu_2 \cdots BrCCH$ and $IAd_2 \cdots BrCCH$ complexes, $\rho_{C \cdots X}$ amounts to 0.010 a.u., whereas 0.017 a.u. in $I \cdots BrCCH$. This is even more evident in systems with iodine, e.g., the $\rho_{C \cdots X}$ value in $I^tBu_2 \cdots ICN$ and $IAd_2 \cdots ICN$ complexes is 0.017 a.u., while, e.g., in the $I \cdots ICN$ complex, it is as much as 0.044 a.u. Thus, apparently, in the case of I^tBu_2 , the greatest length of halogen bonds (if $X \neq Cl$) and their relatively weakest strength result from the large size of highly branched *tert*-butyl groups, which significantly impede the access of XCN and $XCCH$ molecules to the lone electron pair on the carbene carbon atom. The similarly long halogen bonds obtained in the case of IAd_2 (ca. 3.14 Å for XCN and over 3.28 Å for $XCCH$) most likely have the same reason, which is the significant spatial size of the Ad group (however, for the same X -donor, the halogen bond in the $IAd_2 \cdots XD$ complex is about 0.5–0.8 kcal/mol stronger than in $I^tBu_2 \cdots XD$). The complex structures of $I^tBu_2 \cdots BrCN$ and $IAd_2 \cdots BrCN$ shown in Figure 2 represent a case of relatively long and weak halogen bonds, which can probably be attributed to the significant steric hindrance generated by the large tBu and Ad groups. It is worth noting (Table 2) that despite the presence of large substituents, I^tBu_2 and IAd_2 form linear $C \cdots X$ halogen bonds without any exceptions.

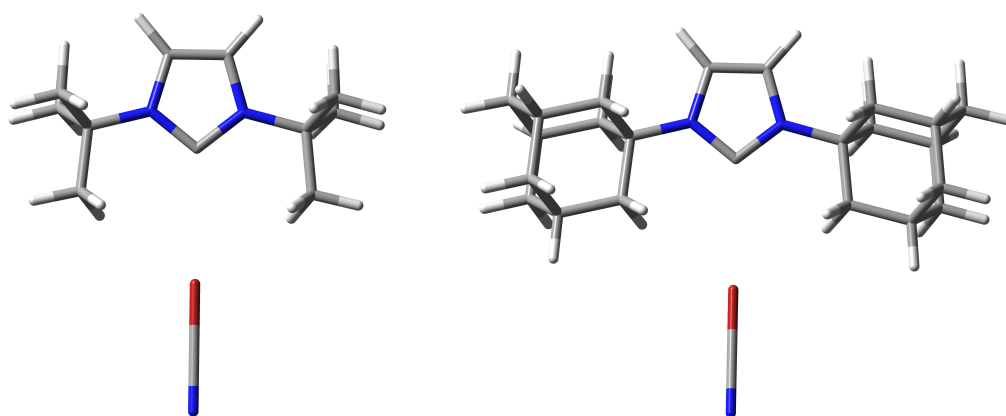


Figure 2. Structures of the $I^tBu_2 \cdots BrCN$ and $IAd_2 \cdots BrCN$ complexes.

However, the steric hindrance of the bulky tBu and Ad groups does not seem to be the sole or even decisive reason for the long and relatively weak halogen bonds in the I^tBu_2 and IAd_2 complexes when we look at the NCI-based [124,125] *s*-isosurfaces of these complexes. Two representative examples ($I^tBu_2 \cdots BrCN$ and $IAd_2 \cdots BrCN$) are shown in Figure 3.

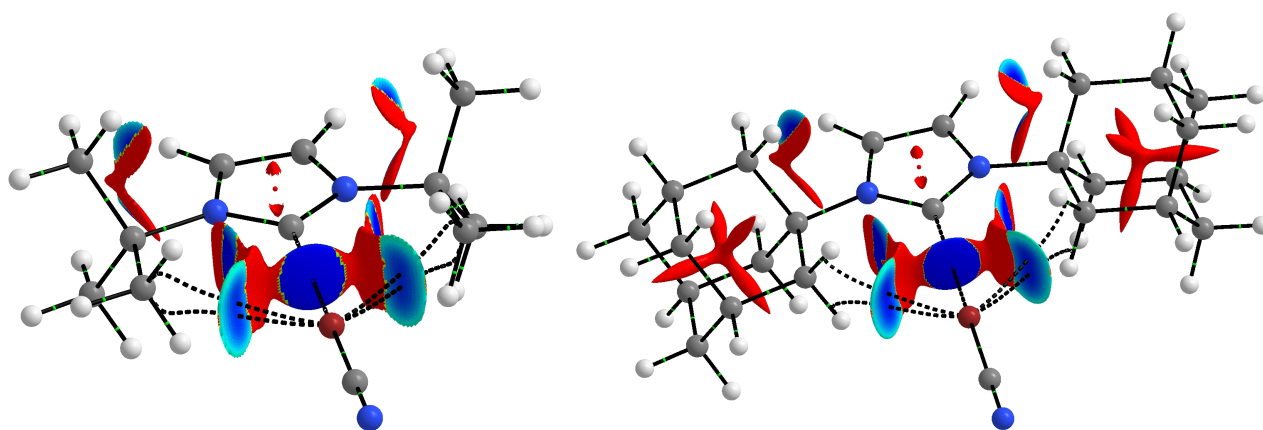


Figure 3. NCI-based s -isosurfaces ($s = 0.5$ a.u.) for the $I^t\text{Bu}_2 \cdots \text{BrCN}$ and $I\text{Ad}_2 \cdots \text{BrCN}$ complexes. Colors are coded according to a common $\text{sgn}(\lambda_2)\rho$ scale (in a.u.): -0.0100 , blue, -0.0075 , cyan; -0.0050 , green; -0.0025 , yellow; and 0.0000 , red. Cutoff of 0.050 a.u. was used for the electron density.

In addition to the clearly visible areas of repulsion (in red) between the bromine atom and either the ^tBu or Ad groups, the subfigures obtained are characterized by the presence of as many as four bond paths between Br and either carbon (in the case of $I^t\text{Bu}_2 \cdots \text{BrCN}$) or hydrogen (in the case of $I\text{Ad}_2 \cdots \text{BrCN}$) atoms, which can be attributed to four $\text{C-H} \cdots \text{Br}$ hydrogen bonds. However, these bonds should be weaker than the $\text{C} \cdots \text{Br}$ halogen bond. The value of the electron density at the critical points of the $\text{C-H} \cdots \text{Br}$ hydrogen bonds is 0.009 a.u. (after using the formula of Emamian et al. [126] this would give the interaction energy of ca. -1.3 kcal/mol), while for the $\text{C} \cdots \text{Br}$ halogen bond, the value of $\rho_{\text{C} \cdots \text{Br}}$ is 0.014 a.u. It is possible that the reason for the rather large $\text{C} \cdots \text{Br}$ distance in these two and similar complexes is the energetically favorable position of the bromine atom in the plane of both C-H bonds forming the $\text{C-H} \cdots \text{Br}$ hydrogen bonds. In other words, the bromine atom is on the prolongation of the C-H bond projections (see Figure 2). Thus, as Figure 3 shows, despite the steric effect of the ^tBu and Ad groups, these groups can also contribute to stabilization, and the resulting complex structure is due to a balance of different effects rather than just one of them. Furthermore, we also note the striking similarity of the NCI-based s -isosurfaces to complexes involving $I^t\text{Bu}_2$ and $I\text{Ad}_2$. The peculiarity is that the hydrogen bonds $\text{C-H} \cdots \text{Br}$ (more generally $\text{C-H} \cdots \text{X}$) in question are characterized by significant values of bond ellipticity. In complexes $I^t\text{Bu}_2 \cdots \text{BrCN}$ and $I\text{Ad}_2 \cdots \text{BrCN}$ shown in Figure 3, these values are 15.5 and 7.2 , respectively, but the value is as high as 148.7 in complex $I^t\text{Bu}_2 \cdots \text{ClCN}$. Such large values of the bond ellipticity of the $\text{C-H} \cdots \text{X}$ hydrogen bonds result from the small distance between the BCPs of these bonds and the ring critical point (RCP) between them.

Interestingly, also the $\text{IMes}_2 \cdots \text{ClCN}$ and $\text{IMes}_2 \cdots \text{ClCCH}$ complexes are characterized by high $d_{\text{C} \cdots \text{Cl}}$ values (3.168 and 3.359 Å, respectively), but in both cases the D_0 values are much higher (9.26 and 5.97 kcal/mol, respectively—which are also the largest D_0 values obtained for ClCN and ClCCH ; see Table 2) than for the corresponding complexes with $I^t\text{Bu}_2$ or $I\text{Ad}_2$. Moreover, the $\rho_{\text{C} \cdots \text{X}}$ values are surprisingly small, only 0.011 and 0.008 a.u., respectively. A significant deviation from linearity (152.9° and 154.6° , respectively) strongly suggests that the reason for such high dissociation energies in both of these complexes is the coexistence of other intermolecular interactions. Indeed, the molecular graphs (see Figure 4) show that ClCN and ClCCH in both complexes are located almost parallel to the ring of one of the mesityl groups and confirm the presence of various intermolecular interactions between these molecules and the Mes group.

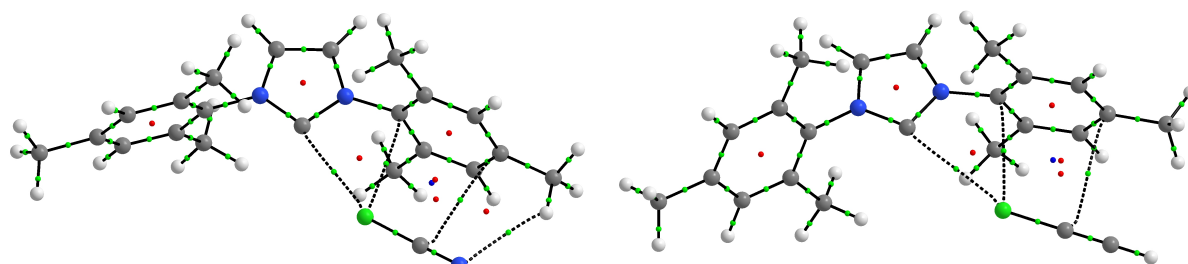


Figure 4. Molecular graphs of the $\text{IMes}_2 \cdots \text{ClCN}$ and $\text{IMes}_2 \cdots \text{ClCCH}$ complexes.

In both cases, the $\text{Cl} \cdots \text{C}$ and $\text{C} \cdots \text{C}$ bond paths are present, which can be understood as the presence of an interaction between the $\text{Cl}-\text{C}$ bond and the π -electron system of the mesityl group. In the case of the complex with ClCN , the $\text{C}-\text{H} \cdots \text{N}$ hydrogen bond path is additionally present. A more complete picture of the interaction between either ClCN or ClCCH and the mesityl group is provided by the NCI-based s -isosurfaces (Figure 5).

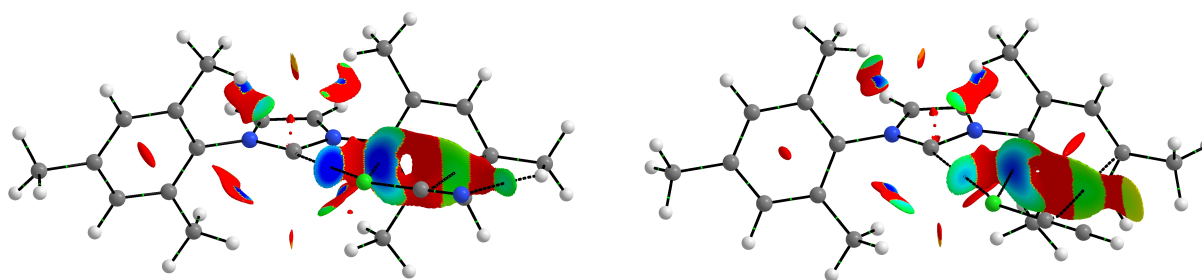


Figure 5. NCI-based s -isosurfaces ($s = 0.5$ a.u.) for the $\text{IMes}_2 \cdots \text{ClCN}$ and $\text{IMes}_2 \cdots \text{ClCCH}$ complexes. Colors are coded according to a common $\text{sgn}(\lambda_2)\rho$ scale (in a.u.): -0.0100 , blue; -0.0075 , cyan; -0.0050 , green; -0.0025 , yellow; and 0.0000 , red. Cutoff of 0.050 a.u. was used for the electron density.

Indeed, they clearly show a large area of intermolecular interaction in this region. This region seamlessly merges with the region (on the left) of the interaction between the carbene carbon atom and the chlorine atom. In the case of the $\text{IMes}_2 \cdots \text{ClCN}$ complex, it is clear that the $\text{Cl} \cdots \text{C}$ secondary interaction is similar in strength to the $\text{C} \cdots \text{Cl}$ halogen bond (the electron density values at the BCPs are 0.010 and 0.011 a.u., respectively) and that both should be much stronger than the $\text{C} \cdots \text{C}$ and $\text{C}-\text{H} \cdots \text{N}$ interactions (ρ_{bcp} values are 0.005 and 0.006 a.u., respectively). Exactly the same pattern of stabilizing interactions also occurs in the $\text{IMes}_2 \cdots \text{ClCCH}$ complex; nevertheless, both $\text{C} \cdots \text{Cl}$ interactions should be weaker (ρ_{bcp} amounts to 0.008 and 0.009 a.u., respectively), though stronger than the $\text{C} \cdots \text{C}$ contacts (0.005 a.u.; one of them (rightmost) is not tracked by a bond path). Interestingly, therefore, it can be seen that in the case of the $\text{IMes}_2 \cdots \text{ClCCH}$ complex, the $\text{C} \cdots \text{Cl}$ halogen bond should be weaker than the interaction between Cl and the mesityl carbon atom directly bonded to the nitrogen atom of the imidazol-2-ylidene ring.

The D_0 values shown in Table 2 clearly indicate that of all the carbenes considered, IMes_2 forms the strongest halogen bonds. Of course, taking into account the fact that the strongest halogen bond is formed by the iodine atom and the XCN molecule, it is not surprising that the strongest halogen bond occurs in the $\text{IMes}_2 \cdots \text{ICN}$ complex (18.71 kcal/mol). Interestingly, despite the large size of the iodine atom, the strongest halogen bond in this complex corresponds to an extremely short $\text{C} \cdots \text{I}$ distance (only 2.541 Å), which is also the shortest halogen bond length in the complexes considered here. This bond is almost linear ($\alpha_{\text{CXC}} = 179.4^\circ$). This complex is also characterized by the highest $\rho_{\text{C} \cdots \text{X}}$ value, amounting to as much as 0.053 a.u. The structure of the $\text{IMes}_2 \cdots \text{ICN}$ complex is shown in Figure 6.

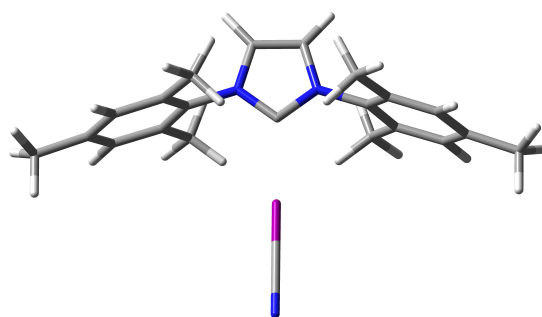


Figure 6. Structure of the $\text{IMes}_2 \cdots \text{ICN}$ complex.

Replacing the iodine atom with a bromine atom and then a chlorine atom causes an increasing deviation from the linearity of the halogen bond, 176.2° for Br, and as already mentioned, only 152.9° for Cl. This result clearly shows that the chlorine atom has the least tendency to form linear or nearly linear halogen bonds. Of course, this is related to the weakest σ -hole. Importantly, it is clearly visible (Table 2) that in many cases, the IDipp_2 carbene forms comparable to IMes_2 strong halogen bonds. For example, in the case of the $\text{IMes}_2 \cdots \text{ICN}$ complex (just discussed) and its counterpart $\text{IDipp}_2 \cdots \text{ICN}$, the dissociation energies are 18.71 and 17.56 kcal/mol, respectively. In the case of the BrCN counterparts, they are 11.18 and 10.95 kcal/mol, respectively, and in the case of BrCCH, the values of D_0 are 7.34 and 7.39 kcal/mol, respectively. It can, therefore, be concluded that despite the slightly different characteristics of the steric hindrance in the bay of the carbene carbon atom, both carbenes, i.e., IMes_2 and IDipp_2 , form (similarly) strong halogen bonds.

It is worth noting that I^tPr_2 also forms short and often strong halogen bonds. Importantly, the relatively small size of the ^tPr group causes that in the $\text{I}^t\text{Pr}_2 \cdots \text{HD}$ complexes the co-existence of other interactions is negligible and therefore the obtained dissociation energy can be identified with the energy of the resulting halogen bond. Of course, the shortest halogen bond is formed with ICN (only 2.552 Å), which is only 0.01 Å longer than in $\text{IMes}_2 \cdots \text{ICN}$. The D_0 value is 17.12 kcal/mol (Table 2).

The $\nabla^2\rho_{\text{C}\cdots\text{X}}$ values also listed in Table 2 show that the considered halogen bonds in the $\text{IR}_2 \cdots \text{XCN}$ and $\text{IR}_2 \cdots \text{XCCH}$ complexes are of the closed-shell type. All halogen bonds involving a chlorine or bromine atom have a (small) positive $H_{\text{C}\cdots\text{X}}$ value. However, this characteristic changes fundamentally for most halogen bonds involving an iodine atom. Namely, this value becomes negative, showing that the given $\text{C}\cdots\text{I}$ halogen bond has a partial covalent character. The most negative $H_{\text{C}\cdots\text{X}}$ values are characteristic of the $\text{IMes}_2 \cdots \text{ICN}$ and $\text{I}^t\text{Pr}_2 \cdots \text{ICN}$ complexes (-0.0109 and -0.0108 a.u., respectively), which also feature similar values of other parameters describing the halogen bond (Table 2). Quite the opposite, for the complexes involving ICN, I^tBu_2 and IAd_2 are the only carbenes giving (slightly) positive $H_{\text{C}\cdots\text{X}}$ values (0.0006 a.u.). This is an indirect confirmation of the relative weakness of the $\text{I}^t\text{Bu}_2 \cdots \text{ICN}$ and $\text{IAd}_2 \cdots \text{ICN}$ complexes.

2.3. Relationships between Physical Quantities

Relatively often in the literature on non-covalent interactions, one can find a statement that the electron density at BCP of a non-covalent bond is linearly correlated with the length of this bond. For this reason, it was tempting to check whether this type of relationship occurs in the $\text{C}\cdots\text{X}$ halogen bonds in the $\text{IR}_2 \cdots \text{XCN}$ and $\text{IR}_2 \cdots \text{XCCH}$ complexes studied here. Of course, this type of correlation was not expected to be perfect since the presence of various accompanying interactions in many of the complexes to some extent affects the value of the $\text{C}\cdots\text{X}$ distance. Indeed, the coefficient of determination R^2 is only 0.832 when all systems are considered together. However, the left subfigure in Figure 7 clearly shows that the reason for such a small value of R^2 is that the corresponding points for the relationship $\rho_{\text{C}\cdots\text{X}}$ vs. $d_{\text{C}\cdots\text{X}}$ are distributed exponentially rather than linearly. Moreover, systems that differ in the type of X should be considered separately.

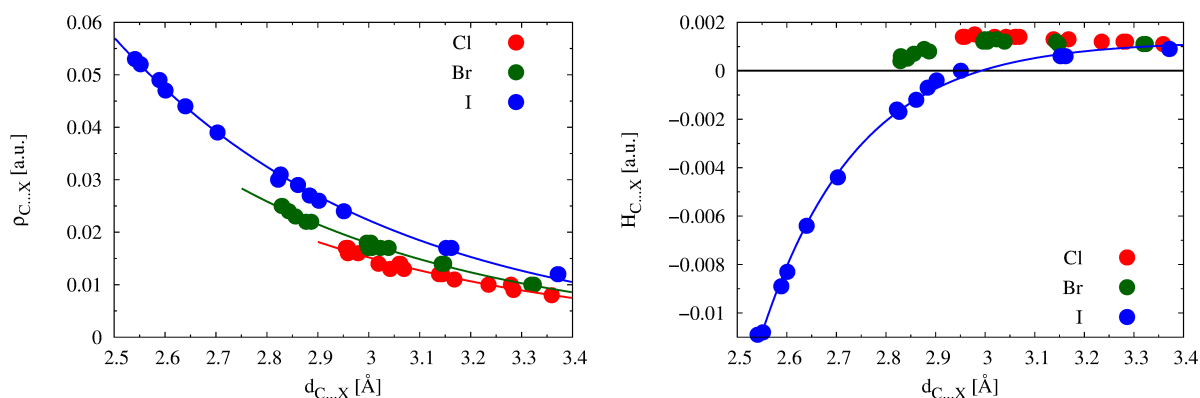


Figure 7. Relationship between either $\rho_{C...X}$ (left) or $H_{C...X}$ (right) and $d_{C...X}$ obtained for the $IR_2 \cdots XCN$ and $IR_2 \cdots XCCH$ ($X = Cl, Br, I$) complexes.

Of course, the corresponding curve for Br is above the curve for Cl, and above it is the curve for I. This is due to the general strength of the halogen bonds $Cl < Br < I$, as mentioned at the beginning of Section 2.2. It is also clear from Figure 7 that the $C \cdots Cl$ halogen bonds are relatively long and with a fairly short range of values, while the length range is larger for $C \cdots Br$, but both of these ranges are definitely overcome by $C \cdots I$, the range of which is up to 0.83 Å, from 2.541 Å to 3.372 Å. However, most importantly in the context of the left subfigure in Figure 7, it is only for small ranges of $d_{C...X}$ (or $\rho_{C...X}$) values that it makes sense to look for reasonably good linear correlations.

In turn, the right subfigure in Figure 7 shows the exponential relationship between $H_{C...X}$ and $d_{C...X}$ determined for complexes where $X = I$. It is clear that similar relationships should be determined for different X separately. This plot is a nice illustration of the previously discussed $H_{C...X}$ values presented in Table 2; namely, all the complexes with Cl or Br feature positive values of $H_{C...X}$. If $X = I$, then most complexes are in the range ± 0.002 a.u. However, the characteristics of the relationship between $H_{C...X}$ and $d_{C...X}$ cause that with the decrease in the distance $C \cdots I$, the value of $H_{C...X}$ decreases rapidly, becoming a significantly negative number, which indicates a significant covalent contribution of the interaction. In extreme cases, an $[IR_2X]^+[D]^-$ ionic pair may be formed [95].

We now show that the R^2 values can also be used to find the carbenes that 'break' the overall linear correlation the most, which is most likely explained by the presence of various secondary interactions whose overall contribution to the complex dissociation energy may be non-negligible. For this purpose, the relationship between $d_{C...X}$ and D_0 was investigated. Of course, as expected, the value of R^2 is small (0.652), indicating that the relationship between $d_{C...X}$ and D_0 is far from linear. However, it is interesting to analyze the obtained R^2 values when linear correlations are made for each of the carbenes separately (see Table 3).

Table 3. Coefficient of determination (R^2) for the relationship between $d_{C...X}$ and D_0 depending on the carbene.

| Carbene | | | | | | | |
|---------|------------------|--------------------------------|--------------------------------|------------------|-------------------|--------------------|------------------|
| I | IMe ₂ | I ^t Pr ₂ | I ^t Bu ₂ | IPh ₂ | IMes ₂ | IDipp ₂ | IAd ₂ |
| 0.964 | 0.984 | 0.993 | 0.255 | 0.937 | 0.828 | 0.932 | 0.274 |

As is clearly seen, the value of R^2 is by far the smallest for I^tBu₂ (0.255) and IAd₂ (0.274). Indeed, both of these carbenes are characterized by the presence of bulky substituents, which, in addition to steric hindrance, can form four hydrogen bonds of the $C-H \cdots X$ type, as exemplified by the I^tBu₂ \cdots BrCN and IAd₂ \cdots BrCN complexes shown in Figure 3. Next in line is IMes₂ (0.828), and indeed, this carbene is also prone to creating

additional accompanying interactions—the best examples of which are the $\text{IMes}_2 \cdots \text{ClCN}$ and $\text{IMes}_2 \cdots \text{ClCCH}$ complexes shown in Figures 4 and 5. A similar analysis was also performed on the X-donor molecule: ClCN (0.099), BrCN (0.713), ICN (0.904), ClCCH (0.417), BrCCH (0.522), ICCH (0.842). The obtained R^2 values suggest that the ClCN molecule is the most ‘problematic’ and that the quality of the linear correlation between $d_{\text{C}\cdots\text{X}}$ and D_0 improves in the order $\text{Cl} \rightarrow \text{Br} \rightarrow \text{I}$, which of course reflects the increasingly developed σ -hole on the halogen atom.

2.4. Halogen Bond vs. Hydrogen Bond

It is instructive to compare the halogen bond characterization discussed here with the hydrogen bond characterization obtained earlier [65] for the same set of carbenes. As has been shown [65], IDipp_2 is prone to forming the strongest complexes with the proton-donor molecule, which was attributed to the co-presence (apart from the dominant (carbene) $\text{C} \cdots \text{H}$ hydrogen bond) of multiple accompanying interactions, such as numerous, e.g., $\text{C-H} \cdots \text{Y}$ hydrogen bonds or $\text{C-H} \cdots \text{H-C}$ contacts, depending on the type of proton-donor molecule. Although the individual interactions are rather very weak, a large number of them can significantly affect the overall strength of the complex. The strongest complex was $\text{IDipp}_2 \cdots \text{HF}$ with the dissociation energy of 19.9 kcal/mol ($\omega\text{B97X-D/6-311++G(d,p)}$), which is only slightly higher than the strongest halogen bond obtained for the $\text{IMes}_2 \cdots \text{ICN}$ complex (ca. 18.7 kcal/mol).

Importantly, it has been shown previously [65] that replacing both hydrogen atoms in the N-H bonds of imidazol-2-ylidene with any substituent under consideration led to a stronger complex with HF, HCN, H_2O , or MeOH. Although this result is in agreement with the lowest nucleophilicity index obtained for I (Table 1), as already discussed, for $\text{IR}_2 \cdots \text{XD}$ complexes, weaker halogen bonds are generally formed by the I^tBu_2 carbene (Table 2). The only exception are systems with chlorine, for which the dissociation energy for I is actually (slightly) lower. For example, for the complexes $\text{I} \cdots \text{ClCN}$ and $\text{I}^t\text{Bu}_2 \cdots \text{ClCN}$, the D_0 values are 5.87 and 6.11 kcal/mol, respectively. Apparently, the presence of branched *tert*-butyl groups hinders the access of larger halogens to the carbene lone electron pair, changing this relationship to the opposite. For example, in the case of ICN , the dissociation energy for I amounts to 14.3 kcal/mol, whereas for I^tBu_2 , this energy is only 9.7 kcal/mol.

2.5. Crystal Structures

In many cases, the interaction of the carbene carbon atom with the halogen atom (especially iodine) is so strong that a C–X bond is formed. An example is 1,3-diethyl-2-iodo-4,5-dimethylimidazolium iodide (HARXAZ) [88], whose lattice fragment is shown in Figure 8. In this case, the carbene carbon forms a $\text{C-I} \cdots \text{I}^-$ link.

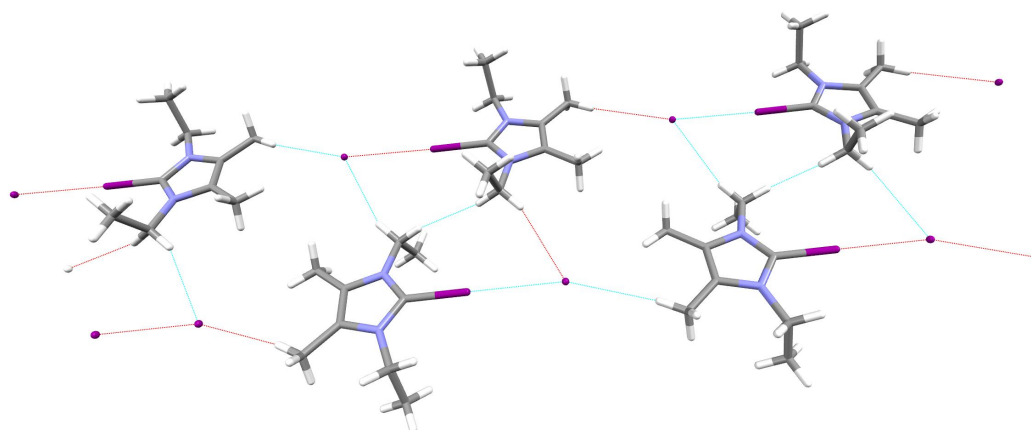


Figure 8. Fragment of the crystal lattice of HARXAZ, i.e., 1,3-diethyl-2-iodo-4,5-dimethylimidazolium iodide. The carbene carbon atom forms a $\text{C-I} \cdots \text{I}^-$ link.

However, using CSD [127], we also managed to find systems in which the presence of a halogen bond to the carbene carbon atom is undeniable. Two such examples are shown in Figure 9.

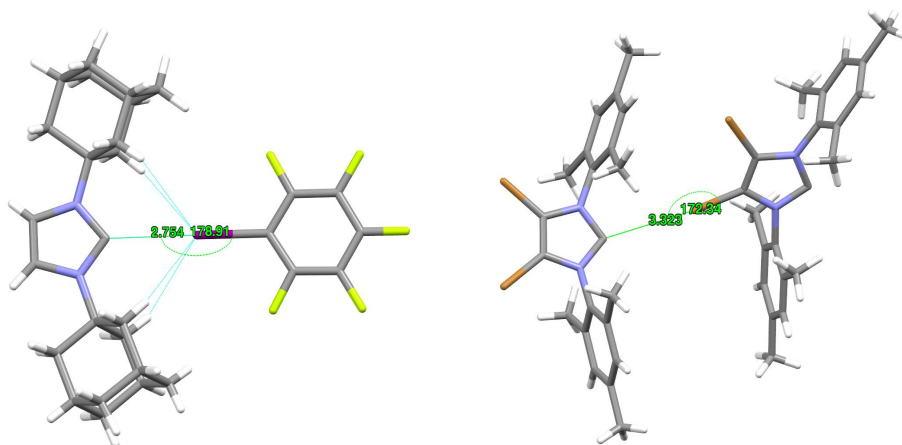


Figure 9. Left: fragment of YABJAM, i.e., (2-(1,3-diadamantylimidazolium))pentafluorophenyl- λ^3 -iodanide tetrahydrofuran solvate (tetrahydrofuran solvate has been removed for better clarity of the figure); right: lattice fragment of 4,5-dibromo-1,3-bis(2,4,6-trimethylphenyl)imidazol-2-ylidene (AHEVEO).

On the left side of Figure 9, a lattice fragment of the previously mentioned (2-(1,3-diadamantylimidazolium))pentafluorophenyl- λ^3 -iodanide tetrahydrofuran solvate present in CSD as YABJAM [87] is shown. In this system, IAd_2 forms a $\text{C} \cdots \text{I}$ type halogen bond with pentafluoriodophenyl. The contact length of $\text{C} \cdots \text{I}$ is only 2.754 Å, much shorter than the theoretical length of halogen bonds in $\text{IAd}_2 \cdots \text{ICN}$ and $\text{IAd}_2 \cdots \text{ICCH}$ (3.152 and 3.371 Å, respectively; Table 2). The $\text{C} \cdots \text{I}-\text{C}$ bridge in this system is almost linear (178.91°). On the right side of Figure 9, a fragment of the crystal lattice of 4,5-dibromo-1,3-bis(2,4,6-trimethylphenyl)imidazol-2-ylidene (AHEVEO) [128] is shown. In this case, the individual molecules are connected by a $\text{C} \cdots \text{Br}$ halogen bond. It is much longer (3.323 Å) than the theoretically determined $\text{C} \cdots \text{Br}$ halogen bond lengths in the $\text{IMes}_2 \cdots \text{BrCN}$ (2.830 Å) and $\text{IMes}_2 \cdots \text{BrCCH}$ (2.999 Å) complexes (Table 2). The $\text{C} \cdots \text{Br}-\text{C}$ bridge in AHEVEO forms an angle of 172.34° .

3. Materials and Methods

Geometries of all the systems (for which charge = 0 and multiplicity = 1) were fully optimized using the global hybrid meta-GGA M06-2X exchange-correlation functional [129,130] of Density Functional Theory [131–133]. Importantly, the M06-2X functional was shown to give accurate geometries and dissociation energies of halogen bonds [134]. Moreover, as recently shown [135], this functional also gives reasonable values for the electron density at the bond critical point—the most important topological parameter in the QTAIM-based [123] analysis. The 6-311++G(d,p) basis set being of the triple-zeta type and containing both polarization and diffuse functions on all atoms [136–140] was used for all atoms but iodine for which the Karlsruhe def2-TZVPD basis set [141–145], taken from Basis Set Exchange (BSE) [146], was used instead. The absence of imaginary frequencies indicated true equilibrium structures every time. Both the geometry optimization and the frequency analysis were performed using the Gaussian 16 (Revision C.01) program [147].

The nucleophilicity index was calculated by four methods (Method I–IV) [122]:

$$\text{Method I: } N_{\text{I}} = E_{\text{HOMO}} - E_{\text{HOMO}}^{\text{TCE}} \quad (1)$$

$$\text{Method II: } N_{\text{II}} = \frac{1}{\omega} \text{ where } \omega = \frac{\mu^2}{2\eta} \quad (2)$$

$$\text{Method III : } N_{\text{III}} = \frac{10}{\omega^-} \text{ where } \omega^- = \frac{I^2}{2(I-A)} \quad (3)$$

$$\text{Method IV : } N_{\text{IV}} = \frac{10}{\omega^-} \text{ where } \omega^- = \frac{(3I+A)^2}{16(I-A)} \quad (4)$$

According to Method I [148], the nucleophilicity index (N_{I}) is simply the difference between the HOMO energies of the test molecule and the reference tetracyanoethylene (TCE) molecule [149,150]. According to Method II, the nucleophilicity index (N_{II}) is determined as the inverse [151] of the electrophilicity index ω [152], where μ is the electronic chemical potential and η is the chemical hardness. Both of these physical quantities were calculated within the finite difference approximation, where $\mu = -\frac{1}{2}(I+A)$ and $\eta = I-A$. Somewhat similarly, Methods III and IV use the inverse of the so-called electrodonating power ω^- [153]. The values of the ionization potential (I) and the electron affinity (A), which were needed to determine the nucleophilicity index according to Methods II–IV, were calculated in the vertical approximation [154], i.e., using the total energies of cations and anions having geometries of neutral carbenes. This approach is much more reasonable than using HOMO and LUMO energies for this purpose. It should be noted that according to Methods II–IV, the unit of the nucleophilicity index is eV^{-1} and eV when the simplest Method I is used.

The dissociation energy was calculated as the difference between the total energy of a complex and the sum of the total energies of isolated subsystems in their own fully optimized structures. Then, the total energies were corrected for the zero-point vibrational energies (ZPVE). Dissociation energies are given as positive values.

Topological analysis of the considered complexes was performed on the basis of Bader's Quantum Theory of Atoms in Molecules (QTAIM) [123]. In addition, this analysis was supplemented with a non-local analysis of weak non-covalent interactions according to the Noncovalent Interaction (NCI) method [124,125]. This method is based on the reduced electron density gradient ($s = 1/(2(3\pi^2)^{1/3})|\nabla\rho|/\rho^{4/3}$) and $\text{sgn}(\lambda_2)\rho$, i.e., the electron density multiplied by the sign of the second eigenvalue of the electron density Hessian matrix (λ_2). As a consequence, NCI allows for displaying individual weak interactions as certain regions of real space rather than as local features of a BCP corresponding to a pairwise interatomic contact. Then, most importantly, these interactions can be easily and visually (by using different colors) separated into attractive (if $\lambda_2 < 0$) and repulsive (if $\lambda_2 > 0$). A common color scale (in a.u.) was used for all systems when producing the NCI-based s -isosurfaces: -0.0100 , blue; -0.0075 , cyan; -0.0050 , green; -0.0025 , yellow; and 0.0000 , red. The QTAIM- and NCI-based calculations were performed using the AIMAll program [155].

4. Conclusions

The article describes halogen bonds involving the carbene carbon atom of imidazol-2-ylidene (I) or its derivatives (IR_2) as a lone electron pair donor. Gradually larger substituents of great experimental importance were taken as R: methyl = Me, *iso*-propyl = ^{*i*}Pr, *tert*-butyl = ^{*t*}Bu, phenyl = Ph, mesityl = Mes, 2,6-diisopropylphenyl = Dipp, 1-adamantyl = Ad. In turn, the halogen atom donors were XCN and XCCH molecules, where X = Cl, Br, I. As a consequence of such a set of carbenes and X-donor molecules, the structures of 48 dimers of the $\text{IR}_2 \cdots \text{XCN}$ and $\text{IR}_2 \cdots \text{XCCH}$ type, bound by the thematic halogen bond $\text{C}_{\text{carbene}} \cdots \text{X}$, have been investigated.

It has been shown that, for a given X-donor, the halogen bond strength increases in the order $\text{Cl} < \text{Br} < \text{I}$ and that the XCN molecule forms stronger complexes than XCCH. It has also been shown that of all the carbenes considered, IMes₂ forms the strongest and also the shortest halogen bonds. Of course, taking into account the above, the strongest ($D_0 = 18.71$ kcal/mol) and at the same time the shortest ($d_{\text{C}\cdots\text{I}} = 2.541$ Å despite the presence of a large iodide atom) halogen bond has been found in the IMes₂ \cdots ICN complex. In many cases, IDipp₂ forms as strong halogen bonds as IMes₂.

In some cases, an extreme example being the complexes $\text{IMes}_2 \cdots \text{ClCN}$ and $\text{IMes}_2 \cdots \text{ClCCH}$, various co-existing secondary interactions are possible, which result in significant non-linearity of the halogen bond. As expected, this tendency is greatest when $X = \text{Cl}$ that can be related to the weakest σ -hole. Noteworthy is the fact that I^iPr_2 forms short and often strong halogen bonds, practically without the participation of additional secondary interactions. For example, in the $\text{I}^i\text{Pr}_2 \cdots \text{ICN}$ complex, $D_0 = 17.12 \text{ kcal/mol}$ and $d_{\text{C}\cdots\text{I}} = 2.552 \text{ \AA}$ only.

Based on the computed values of the nucleophilicity index, I^tBu_2 and IDipp_2 should form the strongest halogen bonds. Surprisingly, however, it has turned out that I^tBu_2 gives the weakest and not the strongest complexes if $X \neq \text{Cl}$. This carbene also forms the longest and always linear halogen bonds. While this finding could easily be attributed to the significant steric hindrance produced by the branched *tert*-butyl groups, it has been shown that an equally important reason could be the possibility of additional stabilization of the complex through the formation of four weak $\text{C-H} \cdots \text{X}$ hydrogen bonds. The same is true for complexes with IAd_2 , which also forms long halogen bonds.

It has also been shown that the relationship between the value of the electron density at the critical point of the $\text{C} \cdots \text{X}$ halogen bond and its length is not linear but rather exponential and only for small ranges of either of these parameters it makes sense to look for a linear relationship. In addition, the relationship should be determined separately for different types of atom X.

Supplementary Materials: The following are available at <https://www.mdpi.com/article/10.3390/ijms24109057/s1>: the fully optimized structures of the investigated complexes.

Funding: This research received no external funding.

Data Availability Statement: The fully optimized structures of the investigated complexes are included in Supplementary Materials. Other data are available from the author upon reasonable request.

Conflicts of Interest: The author declares no conflict of interest.

Abbreviations

The following abbreviations are used in this manuscript:

| | |
|---------------|--------------------------------------|
| XB | halogen bond |
| XD | halogen-donor |
| NHC | N-heterocyclic-carbenes |
| I | imidazol-2-ylidene |
| IR_2 | R-substituted imidazol-2-ylidene |
| Me | methyl group |
| ^iPr | isopropyl group |
| ^tBu | <i>tert</i> -butyl group |
| Ph | phenyl group |
| Mes | mesityl group |
| Dipp | 2,6-diisopropylphenyl group |
| Ad | adamantyl group |
| DFT | Density Functional Theory |
| QTAIM | Quantum Theory of Atoms in Molecules |
| BCP | bond critical point |
| RCP | ring critical point |
| NCI | Noncovalent Interaction (index) |

References

1. Wanzlick, H.W. Aspects of Nucleophilic Carbene Chemistry. *Angew. Chem. Int. Ed. Engl.* **1962**, *1*, 75–80. [[CrossRef](#)]
2. Kirmse, W. *Carbene Chemistry*; Academic Press: Cambridge, MA, USA, 1964.
3. Hubert, A.J. *Catalysis in C₁ Chemistry*; Springer: Dordrecht, The Netherlands, 1983.
4. Schubert, U. *Advances in Metal Carbene Chemistry*; Springer: Dordrecht, The Netherlands, 1989.
5. Bourissou, D.; Guerret, O.; Gabbai, F.P.; Bertrand, G. Stable Carbenes. *Chem. Rev.* **2000**, *100*, 39–91. [[CrossRef](#)] [[PubMed](#)]

6. Bertrande, G. *Carbene Chemistry: From Fleeting Intermediates to Powerful Reagents*; FontisMedia S.A.: Lausanne, Switzerland; Marcel Dekker, Inc.: New York, NY, USA, 2002.
7. Moss, R.A.; Platz, M.S.; Jones, M., Jr. (Eds.) *Reactive Intermediate Chemistry*; John Wiley & Sons, Inc.: Hoboken, NJ, USA, 2005.
8. Carey, F.A.; Sundberg, R.J. *Carbenes, Part B: Reactions and Synthesis. Advanced Organic Chemistry*; Springer: New York, NY, USA, 2007.
9. de Frémont, P.; Marion, N.; Nolan, S.P. Carbenes: Synthesis, properties, and organometallic chemistry. *Coord. Chem. Rev.* **2009**, *253*, 862–892. [[CrossRef](#)]
10. Moss, R.A.; Doyle, M.P. *Contemporary Carbene Chemistry*; John Wiley & Sons, Inc.: Hoboken, NJ, USA, 2013.
11. Herrmann, W.A.; Köcher, C. N-Heterocyclic Carbenes. *Angew. Chem. Int. Ed. Engl.* **1997**, *36*, 2162–2187. [[CrossRef](#)]
12. Nemcsok, D.; Wichmann, K.; Frenking, G. The Significance of π Interactions in Group 11 Complexes with N-Heterocyclic Carbenes. *Organometallics* **2004**, *23*, 3640–3646. [[CrossRef](#)]
13. Scott, N.M.; Nolan, S.P. Stabilization of Organometallic Species Achieved by the Use of N-Heterocyclic Carbene (NHC) Ligands. *Eur. J. Inorg. Chem.* **2005**, 1815–1828. [[CrossRef](#)]
14. Nolan, S.P. *N-Heterocyclic Carbenes in Synthesis*; Wiley-VCH: Weinheim, Germany, 2006.
15. Díez-González, S.; Nolan, S.P. Stereoelectronic parameters associated with N-heterocyclic carbene (NHC) ligands: A quest for understanding. *Coord. Chem. Rev.* **2007**, *251*, 874–883. [[CrossRef](#)]
16. Tonner, R.; Heydenrych, G.; Frenking, G. Bonding Analysis of N-Heterocyclic Carbene Tautomers and Phosphine Ligands in Transition-Metal Complexes: A Theoretical Study. *Chem. Asian J.* **2007**, *2*, 1555–1567. [[CrossRef](#)]
17. Jacobsen, H.; Correa, A.; Poater, A.; Costabile, C.; Cavallo, L. Understanding the M–(NHC) (NHC = N-heterocyclic carbene) bond. *Coord. Chem. Rev.* **2009**, *253*, 687–703. [[CrossRef](#)]
18. Srebro, M.; Michalak, A. Theoretical Analysis of Bonding in N-Heterocyclic Carbene–Rhodium Complexes. *Inorg. Chem.* **2009**, *48*, 5361–5369. [[CrossRef](#)]
19. Nelson, D.J.; Nolan, S.P. Quantifying and understanding the electronic properties of N-heterocyclic carbenes. *Chem. Soc. Rev.* **2013**, *42*, 6723–6753. [[CrossRef](#)] [[PubMed](#)]
20. Hopkinson, M.N.; Richter, C.; Schedler, M.; Glorius, F. An overview of N-heterocyclic carbenes. *Nature* **2014**, *510*, 485–496. [[CrossRef](#)]
21. Bellemin-Laponnaz, S.; Dagorne, S. Group 1 and 2 and Early Transition Metal Complexes Bearing N-Heterocyclic Carbene Ligands: Coordination Chemistry, Reactivity, and Applications. *Chem. Rev.* **2014**, *114*, 8747–8774. [[CrossRef](#)] [[PubMed](#)]
22. Andrada, D.M.; Holzmann, N.; Hamadi, T.; Frenking, G. Direct estimate of the internal π -donation to the carbene centre within N-heterocyclic carbenes and related molecules. *Beilstein J. Org. Chem.* **2015**, *11*, 2727–2736. [[CrossRef](#)] [[PubMed](#)]
23. Nesterov, V.; Reiter, D.; Bag, P.; Frisch, P.; Holzner, R.; Porzelt, A.; Inoue, S. NHCs in Main Group Chemistry. *Chem. Rev.* **2018**, *118*, 9678–9842. [[CrossRef](#)]
24. Santoro, O.; Nahra, F.; Cordes, D.B.; Slawin, A.M.Z.; Nolan, S.P.; Cazin, C.S.J. Synthesis, characterization and catalytic activity of stable [(NHC)H][ZnXY₂] (NHC = N-Heterocyclic carbene, X, Y = Cl, Br) species. *J. Mol. Catal.* **2016**, *423*, 85–91. [[CrossRef](#)]
25. Dagorne, S. Recent Developments on N-Heterocyclic Carbene Supported Zinc Complexes: Synthesis and Use in Catalysis. *Synthesis* **2018**, *50*, 3662–3670. [[CrossRef](#)]
26. Procter, R.J.; Uzelac, M.; Cid, J.; Rushworth, P.J.; Ingleson, M.J. Low-Coordinate NHC–Zinc Hydride Complexes Catalyze Alkyne C–H Borylation and Hydroboration Using Pinacolborane. *ACS Catal.* **2019**, *9*, 5760–5771. [[CrossRef](#)]
27. Dzieszowski, K.; Barańska, I.; Mroczynska, K.; Słotwiński, M.; Rafinski, Z. Organocatalytic Name Reactions Enabled by NHCs. *Materials* **2020**, *13*, 3574. [[CrossRef](#)]
28. Specklin, D.; Fliedel, C.; Dagorne, S. Recent Representative Advances on the Synthesis and Reactivity of N-Heterocyclic-Carbene-Supported Zinc Complexes. *Chem. Rec.* **2021**, *21*, 1130–1143. [[CrossRef](#)]
29. Huang, J.; Stevens, E.D.; Nolan, S.P.; Petersen, J.L. Olefin Metathesis-Active Ruthenium Complexes Bearing a Nucleophilic Carbene Ligand. *J. Am. Chem. Soc.* **1999**, *121*, 2674–2678. [[CrossRef](#)]
30. Scholl, M.; Trnka, T.M.; Morgan, J.P.; Grubbs, R.H. Increased Ring Closing Metathesis Activity of Ruthenium-Based Olefin Metathesis Catalysts Coordinated with Imidazolin-2-ylidene Ligands. *Tetrahedron Lett.* **1999**, *40*, 2247–2250. [[CrossRef](#)]
31. Scholl, M.; Ding, S.; Lee, C.W.; Grubbs, R.H. Synthesis and Activity of a New Generation of Ruthenium-Based Olefin Metathesis Catalysts Coordinated with 1,3-Dimesityl-4,5-dihydroimidazol-2-ylidene Ligands. *Org. Lett.* **1999**, *1*, 953–956. [[CrossRef](#)]
32. Ackermann, L.; Fürstner, A.; Weskamp, T.; Kohl, F.J.; Herrmann, W.A. Ruthenium Carbene Complexes with Imidazolin-2-ylidene Ligands Allow the Formation of Tetrasubstituted Cycloalkenes by RCM. *Tetrahedron Lett.* **1999**, *40*, 4787–4790. [[CrossRef](#)]
33. Kingsbury, J.S.; Harrity, J.P.A.; Bonitatebus, P.J., Jr.; Hoveyda, A.H. A Recyclable Ru-Based Metathesis Catalyst. *J. Am. Chem. Soc.* **1999**, *121*, 791–799. [[CrossRef](#)]
34. Walsh, D.J.; Lau, S.H.; Hyatt, M.G.; Guironnet, D. Kinetic Study of Living Ring-Opening Metathesis Polymerization with Third-Generation Grubbs Catalysts. *J. Am. Chem. Soc.* **2017**, *139*, 13644–13647. [[CrossRef](#)]
35. Leitgeb, A.; Wappel, J.; Slugovc, C. The ROMP toolbox upgraded. *Polymer* **2010**, *51*, 2927–2946. [[CrossRef](#)]
36. Mercks, L.; Albrecht, M. Beyond catalysis: N-heterocyclic carbene complexes as components for medicinal, luminescent, and functional materials applications. *Chem. Soc. Rev.* **2010**, *39*, 1903–1912. [[CrossRef](#)]
37. Visbal, R.; Concepción Gimeno, M. N-heterocyclic carbene metal complexes: Photoluminescence and applications. *Chem. Soc. Rev.* **2014**, *43*, 3551–3574. [[CrossRef](#)]

38. Garrison, J.C.; Youngs, W.J. Ag(I) N-Heterocyclic Carbene Complexes: Synthesis, Structure, and Application. *Chem. Rev.* **2005**, *105*, 3978–4008. [[CrossRef](#)]
39. Hindi, K.M.; Panzner, M.J.; Tessier, C.A.; Cannon, C.L.; Youngs, W.J. The Medicinal Applications of Imidazolium Carbene—Metal Complexes. *Chem. Rev.* **2009**, *109*, 3859–3884. [[CrossRef](#)]
40. Arduengo, A.J., III; Davidson, F.; Krafczyk, R.; Marshall, W.J.; Tamm, M. Adducts of Carbenes with Group II and XII Metallocenes. *Organometallics* **1998**, *17*, 3375–3382. [[CrossRef](#)]
41. Cases, M.; Frenking, G.; Duran, M.; Solà, M. Molecular Structure and Bond Characterization of the Fischer-Type Chromium–Carbene Complexes $(CO)_5Cr = C(X)R$ ($X = H, OH, OCH_3, NH_2, NHCH_3$ and $R = H, CH_3, CH = CH_2, Ph, C \equiv CH$). *Organometallics* **2002**, *21*, 4182–4191. [[CrossRef](#)]
42. Abernethy, C.D.; Baker, R.J.; Cole, M.L.; Davies, A.J.; Jones, C. Reactions of a carbene stabilised indium trihydride complex, $[InH_3\{CN(Mes)-C_2H_2N(Mes)\}]$ Mes = mesityl, with transition metal complexes. *Trans. Metal. Chem.* **2003**, *28*, 296–299. [[CrossRef](#)]
43. Wang, D.; Wurst, K.; Buchmeiser, M.R. N-heterocyclic carbene complexes of Zn(II): Synthesis, X-ray structures and reactivity. *J. Organomet. Chem.* **2004**, *689*, 2123–2130. [[CrossRef](#)]
44. Frenking, G.; Solà, M.; Vyboishchikov, S.F. Chemical bonding in transition metal carbene complexes. *J. Organomet. Chem.* **2005**, *690*, 6178–6204. [[CrossRef](#)]
45. Jensen, T.R.; Schaller, C.P.; Hillmyer, M.A.; Tolman, W.B. Zinc N-heterocyclic carbene complexes and their polymerization of D,L-lactide. *J. Organomet. Chem.* **2005**, *690*, 5881–5891. [[CrossRef](#)]
46. Anantharaman, G.; Elango, K. Synthesis and Characterization of NHC-Stabilized Zinc Aryloxide and Zinc Hydroxyaryloxide. *Organometallics* **2007**, *26*, 1089–1092. [[CrossRef](#)]
47. Radius, U.; Bickelhaupt, F.M. Bonding of Imidazol-2-ylidene Ligands in Nickel Complexes. *Organometallics* **2008**, *27*, 3410–3414. [[CrossRef](#)]
48. Budagumpi, S.; Endud, S. Group XII Metal–N-Heterocyclic Carbene Complexes: Synthesis, Structural Diversity, Intramolecular Interactions, and Applications. *Organometallics* **2013**, *32*, 1537–1562. [[CrossRef](#)]
49. Schnee, G.; Fliedel, C.; Avilés, T.; Dagorne, S. Neutral and Cationic N-Heterocyclic Carbene Zinc Adducts and the $BnOH/Zn(C_6F_5)_2$ Binary Mixture—Characterization and Use in the Ring-Opening Polymerization of β -Butyrolactone, Lactide, and Trimethylene Carbonate. *Eur. J. Inorg. Chem.* **2013**, 3699–3709. [[CrossRef](#)]
50. Fliedel, C.; Vila-Viçosa, D.; Calhorda, M.J.; Dagorne, S.; Avilés, T. Dinuclear Zinc–N-Heterocyclic Carbene Complexes for Either the Controlled Ring-Opening Polymerization of Lactide or the Controlled Degradation of Polylactide Under Mild Conditions. *ChemCatChem* **2014**, *6*, 1357–1367. [[CrossRef](#)]
51. Collins, L.R.; Moffat, L.A.; Mahon, M.F.; Jones, M.D.; Whittlesey, M.K. Lactide polymerisation by ring-expanded NHC complexes of zinc. *Polyhedron* **2016**, *103*, 121–125. [[CrossRef](#)]
52. Tian, J.; Chen, Y.; Vayer, M.; Djurovic, A.; Guillot, R.; Guermazi, R.; Dagorne, S.; Bour, C.; Gandon, V. Exploring the Limits of π -Acid Catalysis Using Strongly Electrophilic Main Group Metal Complexes: The Case of Zinc and Aluminium. *Chem. Eur. J.* **2020**, *26*, 12831–12838. [[CrossRef](#)]
53. Roy, M.M.D.; Baird, S.R.; Ferguson, M.J.; Rivard, E. Toward N-heterocyclic carbene stabilized zinc sulfides. *Mendeleev Commun.* **2021**, *31*, 173–175. [[CrossRef](#)]
54. Jabłoński, M. Study of Beryllium, Magnesium, and Spodium Bonds to Carbenes and Carbodiphosphoranes. *Molecules* **2021**, *26*, 2275. [[CrossRef](#)] [[PubMed](#)]
55. Jabłoński, M. Theoretical Study of N-Heterocyclic-Carbene– ZnX_2 ($X = H, Me, Et$) Complexes. *Materials* **2021**, *14*, 6147. [[CrossRef](#)]
56. Sagan, F.; Mitoraj, M.; Jabłoński, M. Nature of Beryllium, Magnesium, and Zinc Bonds in Carbene $\cdots MX_2$ ($M = Be, Mg, Zn; X = H, Br$) Dimers Revealed by the IQA, ETS-NOCV and LED Methods. *Int. J. Mol. Sci.* **2022**, *23*, 14668. [[CrossRef](#)]
57. Pople, J.A.; Raghavachari, K.; Frisch, M.J.; Binkley, J.S.; Schleyer, P.v.R. Comprehensive Theoretical Study of Isomers and Rearrangement Barriers of Even-Electron Polyatomic Molecules H_mABH_n ($A, B = C, N, O$, and F). *J. Am. Chem. Soc.* **1983**, *105*, 6389–6398. [[CrossRef](#)]
58. Pople, J.A. A Theoretical Search for the Methylene-fluoronium Ylide. *Chem. Phys. Lett.* **1986**, *132*, 144–146. [[CrossRef](#)]
59. Arduengo, A.J., III; Gamper, S.F.; Tamm, M.; Calabrese, J.C.; Davidson, F.; Craig, H.A. A Bis(carbene)–Proton Complex: Structure of a C–H–C Hydrogen Bond. *J. Am. Chem. Soc.* **1995**, *117*, 572–573. [[CrossRef](#)]
60. Alkorta, I.; Elguero, J. Carbenes and Silylenes as Hydrogen Bond Acceptors. *J. Phys. Chem.* **1996**, *100*, 19367–19370. [[CrossRef](#)]
61. Jabłoński, M.; Palusiak, M. Divalent carbon atom as the proton acceptor in hydrogen bonding. *Phys. Chem. Chem. Phys.* **2009**, *11*, 5711–5719. [[CrossRef](#)] [[PubMed](#)]
62. Giffin, N.A.; Makramalla, M.; Hendsbee, A.D.; Robertson, K.N.; Sherren, C.; Pye, C.C.; Masuda, J.D.; Clyburne, J.A.C. Anhydrous TEMPO-H: Reactions of a good hydrogen atom donor with low-valent carbon centres. *Org. Biomol. Chem.* **2011**, *9*, 3672–3680. [[CrossRef](#)]
63. Gerbig, D.; Ley, D. Computational methods for contemporary carbene chemistry. *WIREs Comput. Mol. Sci.* **2013**, *3*, 242–272. [[CrossRef](#)]
64. Samanta, R.C.; De Sarkar, S.; Fröhlich, R.; Grimme, S.; Studer, A. N-Heterocyclic carbene (NHC) catalyzed chemoselective acylation of alcohols in the presence of amines with various acylating reagents. *Chem. Sci.* **2013**, *4*, 2177–2184. [[CrossRef](#)]

65. Jabłoński, M. On the Coexistence of the Carbene···H-D Hydrogen Bond and Other Accompanying Interactions in Forty Dimers of N-Heterocyclic-Carbenes (I, IMe₂, IⁱPr₂, I^tBu₂, IMes₂, IDipp₂, IAd₂; I = imidazol-2-ylidene) and Some Fundamental Proton Donors (HF, HCN, H₂O, MeOH, NH₃). *Molecules* **2022**, *27*, 5712. [[CrossRef](#)]
66. Li, Q.; Wang, H.; Liu, Z.; Li, W.; Cheng, J.; Gong, B.; Sun, J. Ab Initio Study of Lithium-Bonded Complexes with Carbene as an Electron Donor. *J. Phys. Chem. A* **2009**, *113*, 14156–14160. [[CrossRef](#)]
67. Wang, Y.; Xie, Y.; Abraham, M.Y.; Wei, P.; Schaefer, H.F., III; Schleyer, P.v.R.; Robinson, G.H. A Viable Anionic N-Heterocyclic Dicarbene. *J. Am. Chem. Soc.* **2010**, *132*, 14370–14372. [[CrossRef](#)] [[PubMed](#)]
68. Li, Z.F.; Sheng, Y.; Li, H.X. Theoretical prediction characters of unconventional weak bond with carbene as electron donors and Li–Y (Y = OH, H, F, NC and CN) as electron acceptors. *J. Mol. Struct. THEOCHEM* **2010**, *952*, 56–60.
69. Herrmann, W.A.; Runte, O.; Artus, G. Synthesis and structure of an ionic beryllium—“Carbene” complex. *J. Organomet. Chem.* **1995**, *501*, C1–C4. [[CrossRef](#)]
70. Gilliard, R.J., Jr.; Abraham, M.Y.; Wang, Y.; Wei, P.; Xie, Y.; Quillian, B.; Schaefer, H.F., III; Schleyer, P.v.R.; Robinson, G.H. Carbene-Stabilized Beryllium Borohydride. *J. Am. Chem. Soc.* **2012**, *134*, 9953–9955. [[CrossRef](#)]
71. Arrowsmith, M.; Hill, M.S.; Kociok-Köhn, G.; MacDougall, D.J.; Mahon, M.F. Beryllium-Induced C–N Bond Activation and Ring Opening of an N-Heterocyclic Carbene. *Angew. Chem. Int. Ed.* **2012**, *51*, 2098–2100. [[CrossRef](#)]
72. Walley, J.E.; Wong, Y.-O.; Freeman, L.A.; Dickie, D.A.; Gilliard, R.J., Jr. N-Heterocyclic Carbene-Supported Aryl- and Alk-oxides of Beryllium and Magnesium. *Catalysts* **2019**, *9*, 934. [[CrossRef](#)]
73. Arduengo, A.J., III; Dias, H.V.R.; Davidson, F.; Harlow, R.L. Carbene adducts of magnesium and zinc. *J. Organomet. Chem.* **1993**, *462*, 13–18. [[CrossRef](#)]
74. Arrowsmith, M.; Hill, M.S.; MacDougall, D.J.; Mahon, M.F. A Hydride-Rich Magnesium Cluster. *Angew. Chem. Int. Ed.* **2009**, *48*, 4013–4016. [[CrossRef](#)] [[PubMed](#)]
75. Arnold, P.L.; Casely, I.J.; Turner, Z.R.; Bellabarba, R.; Tooze, R.B. Magnesium and zinc complexes of functionalised, saturated N-heterocyclic carbene ligands: Carbene lability and functionalisation, and lactide polymerisation catalysis. *Dalton Trans.* **2009**, 7236–7247. [[CrossRef](#)]
76. Arduengo, A.J., III; Dias, H.V.R.; Calabrese, J.C.; Davidson, F. A Stable Carbene–Alane Adduct. *J. Am. Chem. Soc.* **1992**, *114*, 9724–9725. [[CrossRef](#)]
77. Li, X.-W.; Su, J.; Robinson, G.H. Syntheses and molecular structure of organo-group 13 metal carbene complexes. *Chem. Commun.* **1996**, *23*, 2683–2684. [[CrossRef](#)]
78. Hibbs, D.E.; Hursthouse, M.B.; Jones, C.; Smithies, N.A. Synthesis, crystal and molecular structure of the first indium trihydride complex, [InH₃{CN(Prⁱ)C₂Me₂N(Prⁱ)}]. *Chem. Commun.* **1998**, *8*, 869–870. [[CrossRef](#)]
79. Merceron, N.; Miqueu, K.; Baceiredo, A.; Bertrand, G. Stable (Amino)(phosphino)carbenes: Difunctional Molecules. *J. Am. Chem. Soc.* **2002**, *124*, 6806–6807. [[CrossRef](#)]
80. Wang, Y.; Robinson, G.H. Unique homonuclear multiple bonding in main group compounds. *Chem. Commun.* **2009**, 5201–5213. [[CrossRef](#)] [[PubMed](#)]
81. Del Bene, J.E.; Alkorta, I.; Elguero, J. Carbon–Carbon Bonding between Nitrogen Heterocyclic Carbenes and CO₂. *J. Phys. Chem. A* **2017**, *121*, 8136–8146. [[CrossRef](#)]
82. Liu, M.; Li, Q.; Li, W.; Cheng, J. Carbene tetrel-bonded complexes. *Struct. Chem.* **2017**, *28*, 823–831. [[CrossRef](#)]
83. Wang, Y.; Xie, Y.; Abraham, M.Y.; Gilliard, R.J., Jr.; Wei, P.; Schaefer, H.F., III; Schleyer, P.v.R.; Robinson, G.H. Carbene-Stabilized Parent Phosphinidene. *Organometallics* **2010**, *29*, 4778–4780. [[CrossRef](#)]
84. Abraham, M.Y.; Wang, Y.; Xie, Y.; Wei, P.; Schaefer, H.F., III; Schleyer, P.v.R.; Robinson, G.H. Carbene Stabilization of Diarsenic: From Hypervalency to Allotropy. *Chem. Eur. J.* **2010**, *16*, 432–435. [[CrossRef](#)]
85. Patel, D.S.; Bharatam, P.V. Divalent N(I) Compounds with Two Lone Pairs on Nitrogen. *J. Phys. Chem. A* **2011**, *115*, 7645–7655. [[CrossRef](#)]
86. Zhao, Q.; Feng, D.; Sun, Y.; Hao, J.; Cai, Z. Theoretical Investigations on the Weak Nonbonded C=S···CH₂ Interactions: Chalcogen-Bonded Complexes with Singlet Carbene as an Electron Donor. *Int. J. Quant. Chem.* **2011**, *111*, 3881–3887. [[CrossRef](#)]
87. Arduengo, A.J., III; Kline, M.; Calabrese, J.C.; Davidson, F. Synthesis of a Reverse Ylide from a Nucleophilic Carbene. *J. Am. Chem. Soc.* **1991**, *113*, 9704–9705. [[CrossRef](#)]
88. Kuhn, N.; Kratz, T.; Henkel, G. A Stable Carbene Iodine Adduct: Secondary Bonding in 1,3-Diethyl-2-iodo-4,5-dimethylimidazolium Iodide. *J. Chem. Soc. Chem. Commun.* **1993**, 1778–1779. [[CrossRef](#)]
89. Li, Q.; Wang, Y.; Liu, Z.; Li, W.; Cheng, J.; Gong, B.; Sun, J. An unconventional halogen bond with carbene as an electron donor: An ab initio study. *Chem. Phys. Lett.* **2009**, *469*, 48–51. [[CrossRef](#)]
90. Esrafil, M.D.; Mohammadirad, N. Insights into the strength and nature of carbene···halogen bond interactions: A theoretical perspective. *J. Mol. Model.* **2013**, *19*, 2559–2566. [[CrossRef](#)] [[PubMed](#)]
91. Esrafil, M.D.; Mohammad-Sabet, F.; Esmailpour, P. Theoretical study on cooperative effects between X···N and X···Carbene halogen bonds (X = F, Cl, Br and I). *J. Mol. Model.* **2013**, *19*, 4797–4804. [[CrossRef](#)] [[PubMed](#)]
92. Donoso-Tauda, O.; Jaque, P.; Elguero, J.; Alkorta, I. Traditional and Ion-Pair Halogen-Bonded Complexes Between Chlorine and Bromine Derivatives and a Nitrogen-Heterocyclic Carbene. *J. Phys. Chem. A* **2014**, *118*, 9552–9560. [[CrossRef](#)]
93. Lv, H.; Zhuo, H.-Y.; Li, Q.-Z.; Yang, X.; Li, W.-Z.; Cheng, J.-B. Halogen bonds with N-heterocyclic carbenes as halogen acceptors: A partially covalent character. *Mol. Phys.* **2014**, *112*, 3024–3032. [[CrossRef](#)]

94. Del Bene, J.E.; Alkorta, I.; Elguero, J. Halogen bonding with carbene bases. *Chem. Phys. Lett.* **2017**, *685*, 338–343. [[CrossRef](#)]
95. Grabowski, S.J. Halogen bonds with carbenes acting as Lewis base units: Complexes of imidazol-2-ylidene: Theoretical analysis and experimental evidence. *Phys. Chem. Chem. Phys.* **2023**, *25*, 9636–9647. [[CrossRef](#)]
96. Esrafil, M.D.; Sabouri, A. Carbene–aerogen bonds: An *ab initio* study. *Mol. Phys.* **2017**, *115*, 971–980. [[CrossRef](#)]
97. Hoffmann, R.; Zeiss, G.D.; Van Dine, G.W. The Electronic Structure of Methylenes. *J. Am. Chem. Soc.* **1968**, *90*, 1485–1499. [[CrossRef](#)]
98. Gleiter, R.; Hoffmann, R. On Stabilizing a Singlet Methylene. *J. Am. Chem. Soc.* **1968**, *90*, 5457–5460. [[CrossRef](#)]
99. Baird, N.C.; Taylor, K.F. Multiplicity of the Ground State and Magnitude of the T_1-S_0 Gap in Substituted Carbenes. *J. Am. Chem. Soc.* **1978**, *100*, 1333–1338. [[CrossRef](#)]
100. Harrison, J.F.; Liedtke, R.C.; Liebman, J.F. The Multiplicity of Substituted Acyclic Carbenes and Related Molecules. *J. Am. Chem. Soc.* **1979**, *101*, 7162–7168. [[CrossRef](#)]
101. Mueller, P.H.; Rondan, N.G.; Houk, K.N.; Harrison, J.F.; Hooper, D.; Willen, B.H.; Liebman, J.F. Carbene Singlet–Triplet Gaps. Linear Correlations with Substituent π Donation. *J. Am. Chem. Soc.* **1981**, *103*, 5049–5052. [[CrossRef](#)]
102. Boehme, C.; Frenking, G. Electronic Structure of Stable Carbenes, Silylenes, and Germylenes. *J. Am. Chem. Soc.* **1996**, *118*, 2039–2046. [[CrossRef](#)]
103. Alkorta, I.; Elguero, J. A LFER analysis of the singlet-triplet gap in a series of sixty-six carbenes. *Chem. Phys. Lett.* **2018**, *691*, 33–36. [[CrossRef](#)]
104. Schoeller, W.W. Electrophilicity and nucleophilicity in singlet carbenes. II. Electrophilic selectivity. *Tetrahedron Lett.* **1980**, *21*, 1509–1510. [[CrossRef](#)]
105. Goumri-Magnet, S.; Polishchuck, O.; Gornitzka, H.; Marsden, C.J.; Baceiredo, A.; Bertrand, G. The Electrophilic Behavior of Stable Phosphanylcarbenes Towards Phosphorus Lone Pairs. *Angew. Chem. Int. Ed.* **1999**, *38*, 3727–3729. [[CrossRef](#)]
106. Moss, R.A.; Wang, L.; Cang, H.; Krogh-Jespersen, K. Extremely reactive carbenes: Electrophiles and nucleophiles. *J. Phys. Org. Chem.* **2017**, *30*, e3555. [[CrossRef](#)]
107. Jabłoński, M. The first theoretical proof of the existence of a hydride-carbene bond. *Chem. Phys. Lett.* **2018**, *710*, 78–83. [[CrossRef](#)]
108. Jabłoński, M. In search for a hydride-carbene bond. *J. Phys. Org. Chem.* **2019**, *32*, e3949. [[CrossRef](#)]
109. Yourdkhani, S.; Jabłoński, M. Physical nature of silane···carbene dimers revealed by state-of-the-art *ab initio* calculations. *J. Comput. Chem.* **2019**, *40*, 2643–2652. [[CrossRef](#)] [[PubMed](#)]
110. Metrangolo, P.; Resnati, G. *Halogen Bonding: Fundamentals and Applications*; Mingos, D.M.P., Ed.; Structure and Bonding; Springer: Berlin/Heidelberg, Germany, 2008.
111. Politzer, P.; Murray, J.S.; Clark, T. Halogen bonding: An electrostatically-driven highly directional noncovalent interaction. *Phys. Chem. Chem. Phys.* **2010**, *12*, 7748–7757. [[CrossRef](#)] [[PubMed](#)]
112. Wang, H.; Wang, W.; Jin, W.J. σ -Hole Bond vs. π -Hole Bond: A Comparison Based on Halogen Bond. *Chem. Rev.* **2016**, *116*, 5072–5104. [[CrossRef](#)] [[PubMed](#)]
113. Varadwaj, P.R.; Varadwaj, A.; Marques, H.M. Halogen Bonding: A Halogen-Centered Noncovalent Interaction Yet to Be Understood. *Inorganics* **2019**, *7*, 40. [[CrossRef](#)]
114. Brinck, T.; Murray, J.S.; Politzer, P. Surface Electrostatic Potentials of Halogenated Methanes as Indicators of Directional Intermolecular Interactions. *Int. J. Quant. Chem.* **1992**, *44*, 57–64. [[CrossRef](#)]
115. Clark, T.; Hennemann, M.; Murray, J.S.; Politzer, P. Halogen bonding: The σ -hole. *J. Mol. Model.* **2007**, *13*, 291–296. [[CrossRef](#)]
116. Politzer, P.; Murray, J.S. An Overview of σ -Hole Bonding, an Important and Widely-Occurring Noncovalent Interaction. In *Practical Aspect of Computational Chemistry*; Leszczynski, J., Shukla, M.K., Eds.; Springer: Berlin/Heidelberg, Germany, 2009.
117. Murray, J.S.; Lane, P.; Politzer, P. Expansion of the σ -hole concept. *J. Mol. Model.* **2009**, *15*, 723–729. [[CrossRef](#)]
118. Mallada, B.; Gallardo, A.; Lamanec, M.; de la Torre, B.; Špirko, V.; Hobza, P.; Jelinek, P. Real-space imaging of anisotropic charge of σ -hole by means of Kelvin probe force microscopy. *Science* **2021**, *374*, 863–867. [[CrossRef](#)]
119. Sanyal, S.; Esterhuysen, C. Nature of halogen bond adducts of carbones with XCF_3 ($X = Cl, Br, I$) species. *Polyhedron* **2021**, *200*, 115107. [[CrossRef](#)]
120. Frosch, J.; Koneczny, M.; Bannenberg, T.; Tamm, M. Halogen Complexes of Anionic N-Heterocyclic Carbenes. *Chem. Eur. J.* **2021**, *27*, 4349–4363. [[CrossRef](#)] [[PubMed](#)]
121. Savin, K.A. *Writing Reaction Mechanisms in Organic Chemistry*; Elsevier Inc.: Amsterdam, The Netherlands, 2015. [[CrossRef](#)]
122. Pratihari, S.; Roy, S. Nucleophilicity and Site Selectivity of Commonly Used Arenes and Heteroarenes. *J. Org. Chem.* **2010**, *75*, 4957–4963. Erratum in *J. Org. Chem.* **2011**, *76*, 4219–4219. [[CrossRef](#)]
123. Bader, R.F.W. *Atoms in Molecules: A Quantum Theory*; Oxford University Press: New York, NY, USA, 1990.
124. Johnson, E.R.; Keinan, S.; Mori-Sánchez, P.; Contreras-García, J.; Cohen, A.J.; Yang, W. Revealing Noncovalent Interactions. *J. Am. Chem. Soc.* **2010**, *132*, 6498–6506. [[CrossRef](#)]
125. Contreras-García, J.; Johnson, E.R.; Keinan, S.; Chaudret, R.; Piquemal, J.-P.; Beratan, D.N.; Yang, W. NCIPLOT: A Program for Plotting Noncovalent Interaction Regions. *J. Chem. Theory Comput.* **2011**, *7*, 625–632. [[CrossRef](#)]
126. Emamian, S.; Lu, T.; Kruse, H.; Emamian, H. Exploring Nature and Predicting Strength of Hydrogen Bonds: A Correlation Analysis Between Atoms-in-Molecules Descriptors, Binding Energies, and Energy Components of Symmetry-Adapted Perturbation Theory. *J. Comput. Chem.* **2019**, *40*, 2868–2881. [[CrossRef](#)] [[PubMed](#)]

127. Groom, C.R.; Bruno, I.J.; Lightfoot, M.P.; Ward, S.C. The Cambridge Structural Database. *Acta Cryst.* **2016**, *B72*, 171–179. [[CrossRef](#)] [[PubMed](#)]
128. Cole, M.L.; Jones, C.; Junk, P.C. Studies of the reactivity of *N*-heterocyclic carbenes with halogen and halide sources. *New J. Chem.* **2002**, *26*, 1296–1303. [[CrossRef](#)]
129. Zhao, Y.; Truhlar, D. The M06 suite of density functionals for main group thermochemistry, thermochemical kinetics, noncovalent interactions, excited states, and transition elements: Two new functionals and systematic testing of four M06-class functionals and 12 other functionals. *Theor. Chem. Acc.* **2008**, *120*, 215–241.
130. Peverati, R.; Truhlar, D.G. Quest for a universal density functional: The accuracy of density functionals across a broad spectrum of databases in chemistry and physics. *Philos. Trans. R. Soc. A* **2014**, *372*, 20120476. [[CrossRef](#)] [[PubMed](#)]
131. Hohenberg, P.; Kohn, W. Inhomogeneous Electron Gas. *Phys. Rev.* **1964**, *136*, B864–B871. [[CrossRef](#)]
132. Kohn, W.; Sham, L.J. Self-Consistent Equations Including Exchange and Correlation Effects. *Phys. Rev.* **1965**, *140*, A1133–A1138. [[CrossRef](#)]
133. Parr, R.G.; Yang, W. *Density-Functional Theory of Atoms and Molecules*; Oxford University Press: New York, NY, USA, 1989.
134. Kozuch, S.; Martin, J.M.L. Halogen Bonds: Benchmarks and Theoretical Analysis. *J. Chem. Theory Comput.* **2013**, *9*, 1918–1931. [[CrossRef](#)] [[PubMed](#)]
135. Domagała, M.; Jabłoński, M.; Dubis, A.T.; Zabel, M.; Pfitzner, A.; Palusiak, M. Testing of Exchange-Correlation Functionals of DFT for a Reliable Description of the Electron Density Distribution in Organic Molecules. *Int. J. Mol. Sci.* **2022**, *23*, 14719. [[CrossRef](#)] [[PubMed](#)]
136. Krishnan, R.; Binkley, J.S.; Seeger, R.; Pople, J.A. Self-consistent molecular orbital methods. XX. A basis set for correlated wave functions. *J. Chem. Phys.* **1980**, *72*, 650–654. [[CrossRef](#)]
137. McLean, A.D.; Chandler, G.S. Contracted Gaussian basis sets for molecular calculations. I. second row atoms, $Z = 11$ –18. *J. Chem. Phys.* **1980**, *72*, 5639–5648. [[CrossRef](#)]
138. Curtiss, L.A.; McGrath, M.P.; Blandeau, J.-P.; Davis, N.E.; Binning, R.C., Jr.; Radom, L. Extension of Gaussian-2 theory to molecules containing third-row atoms Ga–Kr. *J. Chem. Phys.* **1995**, *103*, 6104–6113. [[CrossRef](#)]
139. Frisch, M.J.; Pople, J.A.; Binkley, J.S. Self-consistent molecular orbital methods 25. Supplementary functions for Gaussian basis sets. *J. Chem. Phys.* **1984**, *80*, 3265–3269. [[CrossRef](#)]
140. Clark, T.; Chandrasekhar, J.; Spitznagel, G.W.; Schleyer, P.v.R. Efficient Diffuse Function-Augmented Basis Sets for Anion Calculations. III. The 3–21+G Basis Set for First-Row Elements, Li–F. *J. Comput. Chem.* **1983**, *4*, 294–301. [[CrossRef](#)]
141. Schäfer, A.; Horn, H.; Ahlrichs, R. Fully optimized contracted Gaussian basis sets for atoms Li to Kr. *J. Chem. Phys.* **1992**, *97*, 2571–2577. [[CrossRef](#)]
142. Schäfer, A.; Huber, C.; Ahlrichs, R. Fully optimized contracted Gaussian basis sets of triple zeta valence quality for atoms Li to Kr. *J. Chem. Phys.* **1994**, *100*, 5829–5835. [[CrossRef](#)]
143. Weigend, F.; Furche, F.; Ahlrichs, R. Gaussian basis sets of quadruple zeta valence quality for atoms H–Kr. *J. Chem. Phys.* **2003**, *119*, 12753–12762. [[CrossRef](#)]
144. Weigend, F.; Ahlrichs, R. Balanced basis sets of split valence, triple zeta valence and quadruple zeta valence quality for H to Rn: Design and assessment of accuracy. *Phys. Chem. Chem. Phys.* **2005**, *7*, 3297–3305. [[CrossRef](#)]
145. Weigend, F. Accurate Coulomb-fitting basis sets for H to Rn. *Phys. Chem. Chem. Phys.* **2006**, *8*, 1057–1065. [[CrossRef](#)] [[PubMed](#)]
146. Pritchard, B.P.; Altarawy, D.; Didier, B.; Gibson, T.D.; Windus, T.L. New Basis Set Exchange: An Open, Up-to-Date Resource for the Molecular Sciences Community. *J. Chem. Inf. Model.* **2019**, *59*, 4814–4820. [[CrossRef](#)] [[PubMed](#)]
147. Frisch, M.J.; Trucks, G.W.; Schlegel, H.B.; Scuseria, G.E.; Robb, M.A.; Cheeseman, J.R.; Scalmani, G.; Barone, V.; Petersson, G.A.; Nakatsuji, H.; et al. *Gaussian 16, Revision C.01*; Gaussian, Inc.: Wallingford, CT, USA, 2019.
148. Contreras, R.; Andres, J.; Safont, V.S.; Campodonico, P.; Santos, J.G. A Theoretical Study on the Relationship between Nucleophilicity and Ionization Potentials in Solution Phase. *J. Phys. Chem. A* **2003**, *107*, 5588–5593. [[CrossRef](#)]
149. Domingo, L.R.; Chamorro, E.; Perez, P. Understanding the Reactivity of Captodative Ethylenes in Polar Cycloaddition Reactions. A Theoretical Study. *J. Org. Chem.* **2008**, *73*, 4615–4624. [[CrossRef](#)] [[PubMed](#)]
150. Domingo, L.R.; Pérez, P. The nucleophilicity *N* index in organic chemistry. *Org. Biomol. Chem.* **2011**, *9*, 7168–7175. [[CrossRef](#)]
151. Chattaraj, P.K.; Maiti, B. Reactivity Dynamics in Atom–Field Interactions: A Quantum Fluid Density Functional Study. *J. Phys. Chem. A* **2001**, *105*, 169–183. [[CrossRef](#)]
152. Parr, R.G.; Szentpaly, L.V.; Liu, S. Electrophilicity Index. *J. Am. Chem. Soc.* **1999**, *121*, 1922–1924. [[CrossRef](#)]
153. Gazquez, J.L.; Cedillo, A.; Vela, A.J. Electrodonating and Electroaccepting Powers. *Phys. Chem. A* **2007**, *111*, 1966–1970. [[CrossRef](#)]
154. Politzer, P.; Murray, J.S. Electronegativity—A perspective. *J. Mol. Model.* **2018**, *24*, 214. [[CrossRef](#)]
155. Keith, T.A. *AIMAll*; Version 15.05.18; TK Gristmill Software: Overland Park, KS, USA, 2015. Available online: aim.tkgristmill.com (accessed on 17 September 2022).

Disclaimer/Publisher’s Note: The statements, opinions and data contained in all publications are solely those of the individual author(s) and contributor(s) and not of MDPI and/or the editor(s). MDPI and/or the editor(s) disclaim responsibility for any injury to people or property resulting from any ideas, methods, instructions or products referred to in the content.